A SYSTEMATIC STUDY OF A NOVEL TWO-PHASE SHIP PROPULSOR

Virgil Glenn Cox

A SYSTEMATIC STUDY OF A NOVEL TWO-PHASE SHIP PROPULSOR

by

VIRGIL Glenn COX

B.S., Massachusetts Institute of Technology

(1962)

SUBMITTED IN PARTIAL FULFILLMENT OF THE

REQUIREMENTS FOR THE DEGREE OF

OCEAN ENGINEER

at the

MASSACHUSETTS INSTITUTE OF TECHNOLOGY

June, 1972

A SYSTEMATIC STUDY OF A NOVEL TWO-PHASE SHIP PROPULSOR

by

VIRGIL G. COX

Submitted to the Department of Ocean Engineering on May 12, 1972, in partial fulfillment of the requirements for the degree of Ocean Engineer.

ABSTRACT

A two-phase air-water propulsion system was studied to establish the scaling laws and to determine the efficiency. A calculational method which separates frictional, residuary and air flow associated forces was postulated and physical models were built and tested in a towing tank to provide data for verification of the postulate. Because of the poor quality of the data, the strongest statement that can be made at this time is that the postulated method of separation of forces holds promise and that the system can be expected to have an efficiency (exclusive of power plant and piping, etc.) of about 20%.

Some of the special features and potential areas of application of the two-phase propulsor are discussed. The experimental methodology was examined in light of the results achieved by its use and it was concluded that the experimental procedure needed improvement. Suggestions for further work in the field are given.

Thesis Supervisor: Chryssostomos Chryssostomidis

Title: Assistant Professor of Ocean Engineering

ACKNOWLEDGEMENTS

The author wishes to express his deep appreciation to his thesis advisor, Professor Chryssostomidis, for his constant encouragement, assistance and concern throughout this investigation and in the writing of the thesis. Without his skillful guidance this work could not have been completed.

Special thanks are due to Mr. William Fulton for the use of his model and his continuous interest in the project.

I wish to thank my wife, Patricia, for her help, patience, understanding and tolerance during the course of this study.

The skill and expertise of Mrs. Shirley Price ("Sam") in typing and correcting this thesis are gratefully appreciated.

Finally, the author wishes to thank the Massachusetts Institute of Technology for the use of the Ship Model Towing Tank and the United States Navy for funding of this project.

TABLE OF CONTENTS

Chapter Number		Page
	TITLE PAGE	1
	ABSTRACT	2
	ACKNOWLEDGEMENTS	3
	TABLE OF CONTENTS	4
	LIST OF SYMBOLS	6
	LIST OF FIGURES	9
	LIST OF TABLES	11
I.	INTRODUCTION	13
II.	STATE OF THE ART	18
A.	THEORETICAL	18
B.	EXPERIMENTAL	20
III.	THEORY	22
IV.	EXPERIMENTAL PROCEDURE	26
A.	EQUIPMENT	26
B.	OPERATIONAL PROCEDURE	31
C.	ANALYTIC PROCEDURE	33
	1. BARE HULL RESISTANCE COEFFICIENT	33
	2. BOLLARD PULL TEST	34
	3. RAMP DRAG	35
	4. THRUST PROVIDED BY THE TWO-PHASE PROPULSION SYSTEM	35
	5. SELF-PROPELLED MODEL TESTS	36
V.	EXPERIMENTAL RESULTS	39
A.	ESTABLISHMENT OF FROUDE SCALING OF THE MODELS	39

CONTENTS

		Page
	B. BOLLARD PULL TESTS	44
	C. DETERMINATION OF THE RAMP DRAG	56
	D. SELF-PROPELLED MODEL TESTS	63
	E. THRUST COEFFICIENT, AIR FLOW RESISTANCE COEFFICIENT, EFFICIENCY	90
VI.	DISCUSSION AND CONCLUSIONS	96
	A. EQUIPMENT AND PROCEDURES	96
	B. RESULTS	98
VII.	APPLICATIONS, ENGINEERING CONSIDERATIONS, AND SUGGESTIONS	101
	BIBLIOGRAPHY	105
	APPENDICES	
	A. OVERVIEW OF KOSTILAINEN'S THEORY FOR TWO-PHASE AIR-WATER PROPULSION SYSTEM	106
	B. SAMPLE DETAILED CALCULATION	108

LIST OF SYMBOLS

Symbol	Name
B	Beam of the Vessel
B_c	Breadth of the Channel
C_B	Blockage Coefficient
C_{BH}	Total Resistance Coefficient with no Air Flowing
C_F	Frictional Resistance Coefficient
C_p	Prismatic Coefficient
C_R	Residuary Resistance Coefficient
C_{RD}	Ramp Drag Resistance Coefficient
C_T	Total Resistance Coefficient
C_{TS}	Nondimensional Calculated Force
C_ϕ	Air Flow Resistance Coefficient
D_T	Total Resistance
F	Froude Number
F_I	F_I=Calculated Force on the Ramp Parallel to the Ship's Fore and Aft Axis
F_{nh}	Kostilainen's Froude Number
g	Acceleration of Gravity
h	Depth of orifices
L	Water Line Length
log	Logarithm to the Base Ten
N_B	Number of Orifices per Unit Breadth
P_1	Measured Dynamic Pressure on the Ramp
P_2	Measured Dynamic Pressure on the Ramp
P_3	Measured Dynamic Pressure on the Ramp

Symbol	Name
P_4	Measured Pressure Above the Air Chamber
R	Reynolds Number
R_D	Ramp Drag (Bare Hull)
S	Wetted Surface Area
Step Corr	Dynamic Force Exerted on the Step
T	Total Thrust Created by the Two-Phase Propulsion System Along the Ship's Fore and Aft Axis
T_A	Apparent Thrust, the Total Bare Hull Resistance Minus the Measured Apparent Resistance of the Hull When Air is Flowing
T_m	Measured Resistance of the Hull when Air is Flowing
U	Velocity of the Model
U_L	Velocity of the Liquid at the Orifice
U_2	Liquid Velocity Leaving the Channel
V_G	Volumetric Air Flow Rate
V_L	Amount of Liquid Accelerated
β	Angle the Ramp Makes with the Water Surface
δ	Inner Diameter of Air Supply Pipe
δ_o	Diameter of an Orifice
Δ	Height of Step
η	Efficiency of the Two-Phase Propulsion System (Propulsor Only)
η_J	Ratio of the Increase of Kinetic Energy of the Liquid to the Loss of Potential Energy of the Air
μ	Dynamic Viscosity of the Liquid
ν	Viscosity of the Liquid
ρ	Mass Density of the Liquid

Symbol	Name
σ	Surface Tension of the Liquid
ϕ	Nondimensional Air Flow Rate
ϕ_K	Kostilainen's Nondimensional Air Flow Rate
∇	Displacement

LIST OF FIGURES

Figure Number	Title	Page
1.	Views of the L = 6.75 ft. Hull	16
2.	Lines Drawing	27
3.	Residuary Resistance Coefficient, C_R, versus Froude Number, F	40
4.	Bollard Pull Test Pressure Distribution as a Function of the Air Flow Rate for Model A.	45
5.	Bollard Pull Test Pressure Distribution as a Function of the Air Flow Rate for Model B.	46
6.	Bollard Pull Test Pressure Distribution as a Function of Position for Model A.	47
7.	Bollard Pull Test Pressure Distribution as a Function of Position for Model B.	48
8.	Bollard Pull Test Calculated and Measured Forces as a Function of Air Flow Rate for Model A.	50
9.	Bollard Pull Test Calculated and Measured Forces as a Function of Air Flow Rate for Model B.	51
10.	Bare Hull Ramp Drag Pressure Distribution as a Function of Position for Model A.	57
11.	Bare Hull Ramp Drag Pressure Distribution as a Function of Position for Model B.	58
12.	Ramp Drag Coefficient, C_{RD}, versus Froude Number, F.	59
13.	Self-Propelled Test: Apparent Hull Resistance, T_m, as a Function of the Air Flow Rate for Model A.	64
14.	Self-Propelled Test: Apparent Hull Resistance, T_m, as a Function of the Air Flow Rate for Model B.	65
15.	Froude Number of the Self-Propelled Velocity, F, as a Function of Nondimensional Air Flow Rate, ϕ.	69
16.	C_{TA} versus Froude Number, F.	70

Figure Number	Title	Page
17.	C_{TS} versus Froude Number, F.	91
18.	Air Flow Resistance Coefficient, C_{ϕ}, versus Froude Number, F.	92
19.	Efficiency, η, versus Froude Number, F.	94
20.	Momentum Balance for a Two-Phase Propulsor	110

LIST OF TABLES

Table Number	Title	Page
1.	Model Parameters	28
2.	Bare Hull Resistance, Model A.	42
3.	Bare Hull Resistance, Model B.	43
4.	Bollard Pull Test, Model A.	54
5.	Bollard Pull Test, Model B.	55
6.	Bare Hull Ramp Drag, Model A.	61
7.	Bare Hull Ramp Drag, Model B.	62
8.	Self-Propelled Test: Apparent Hull Resistance, T_m, Model L = 4.5 ft.	66
9.	Self-Propelled Test: Apparent Hull Resistance, T_m, Model L = 6.75 ft.	67
10.	Self-Propelled Model Tests: Model L = 4.5 ft., Velocity = 0.610 KTS	72
11.	Self-Propelled Model Tests: Model L = 4.5 ft., Velocity = 0.610 KTS.	73
12.	Self-Propelled Model Tests, Model L = 4.5 ft., Velocity = 0.901 KTS	74
13.	Self-Propelled Model Tests, Model L = 4.5 ft., Velocity = 0.901 KTS	75
14.	Self-Propelled Model Tests, Model L = 4.5 ft., Velocity = 1.201 KTS	76
15.	Self-Propelled Model Tests, Model L = 4.5 ft., Velocity = 1.201 KTS	77
16.	Self-Propelled Model Tests, Model L = 4.5 ft., Velocity = 1.501 KTS	78
17.	Self-Propelled Model Tests, Model L = 4.5 ft., Velocity = 1.501 KTS	79
18.	Self-Propelled Model Tests, Model L = 6.75 ft., Velocity = 1.006 KTS	80

Table Number	Title	Page
19.	Self Propelled Model Tests, Model L = 6.75 ft., Velocity = 1.006 KTS	81
20.	Self-Propelled Model Tests, Model L = 6.75 ft., Velocity = 1.351 KTS	82
21.	Self-Propelled Model Tests, Model L = 6.75 ft., Velocity = 1.351 KTS	83
22.	Self-Propelled Model Tests, Model L = 6.75 ft., Velocity = 1.510 KTS	84
23.	Self-Propelled Model Tests, Model L = 6.75 ft., Velocity = 1.510 KTS	85
24.	Self-Propelled Model Tests, Model L = 6.75 ft., Velocity = 1.645 KTS	86
25.	Self-Propelled Model Tests, Model L = 6.75 ft., Velocity = 1.645 KTS	87
26.	Self-Propelled Model Tests, Model L = 6.75 ft., Velocity = 1.985 KTS	88
27.	Self-Propelled Model Tests, Model L = 6.75 ft., Velocity = 1.985 KTS	89

I. INTRODUCTION

In recent years several novel ship propulsion systems have been proposed, tested and some have been utilized in full scale. One of the propulsion systems that has been proposed recently, henceforth referred to as a two-phase propulsion system, is the subject of study of this thesis.

Mr. William Fulton has applied for patent rights for this unique propulsion system which consists of air under pressure being forced through an orifice, located approximately amidships at the bottom of ths ship, into a channel which conducts the air to the stern of the ship. The bottom and the sides of the aft part of the ship and the water beneath the ship form the sides of the channel. The channel is on an angle so that as the air-water mixture moves aft it also rises toward the surface of the water.

Professor S. Schuster was the first to study the theory of the two-phase propulsion system and published his results in 1961.[1] Professor Kostilainen has done considerable experimental work on this type of propulsion system and has repcrted his results in several papers.[2, 3] The results of Kostilainen's work are restricted in application but the work has accomplished the following:

(1) The dimensional analysis of the problem and the establishment of some useful dimensionless ratios.

(2) The calculation of the momentum and energy balance equations which identify some of the functional relationships which govern the phenomenon under investigation.

(3) The measurement of the air-flow rate and the apparent resistance of the model with the propulsor operating for two geosims which had a scale factor of four. (The waterline length of the small model was 1.6 meters.) The apparent resistance differs from the total resistance by the amount of thrust developed by the propulsor.

(4) The generation of data and presentation of some of the theory of bubble formation and spreading in the channel.

The major restriction of Kostilainen's work is that although models of two different sizes had been studied, no scaling law was postulated by Kostilainen. In addition the results published do not allow other researchers to postulate such a scaling law and be in a position to verify it. In view of the fact that what is of importance is the behavior of the full sized ship, it was concluded that a study that would permit the establishment of such a scaling law was fully justified.

The proposed study involves:

(1) The formation of a mathematical model that interrelates the critical parameters that describe the phenomenon under investigation and permits the prediction of the full scale ship.

(2) Model testing is to be used to verify the proposed mathematical model.

(3) The comparison of the performance of the proposed propulsion system with the known performance of other propulsion systems.

It should be noted that attempts to calculate thrust from first principles of hydrodynamics were not successful. Therefore it was decided that an experimental approach would be used.

Mr. Fulton had a rough, three-foot model which he had used as the

basis for his patent application and which he was willing to provide for use in this thesis work. His model was faired and slightly modified and a geosim (Model A) with a 1.5 scale factor was built and the two models were tested without air in the M.I.T. towing tank. (For details of Model A see Ship Model, Chapter IV, Section A.) The tests proved that the original model which was operating at a Reynold's number of between 10^5 and 8×10^5 could not be driven into a turbulent flow and the resulting drag measurements could not be compared to those of the larger model. Therefore an even larger model (Model B) was built, again on a scale factor of 1.5. The two models, A and B, used in the final comparison tests, were therefore 4.5 feet and 6.75 feet in length respectively.

Figure 1 shows the geometric configuration studied in this work. The model is bottom up in the pictures. Air under pressure enters the air chamber and passes out the astern opening into the channel. As it passes up the channel toward the stern it imparts momentum to the adjacent water and thus creates a reaction force on the ramp, thus propelling the model.

Observations made through the glass wall of the towing tank indicate that two modes of operation occur. One, at low air flow, is characterized by bubbles passing up the channel. The second, at higher air-flow rates, is characterized by the establishment of waves traveling up the channel. Of course, there is a range of air flows which displays characteristics of both these modes. If the air-flow rate is increased to a high enough value some of the air will start escaping from the air chamber and rise up outside the ship and provide no propulsion force.

Chapter II gives a more detailed study of the theoretical and

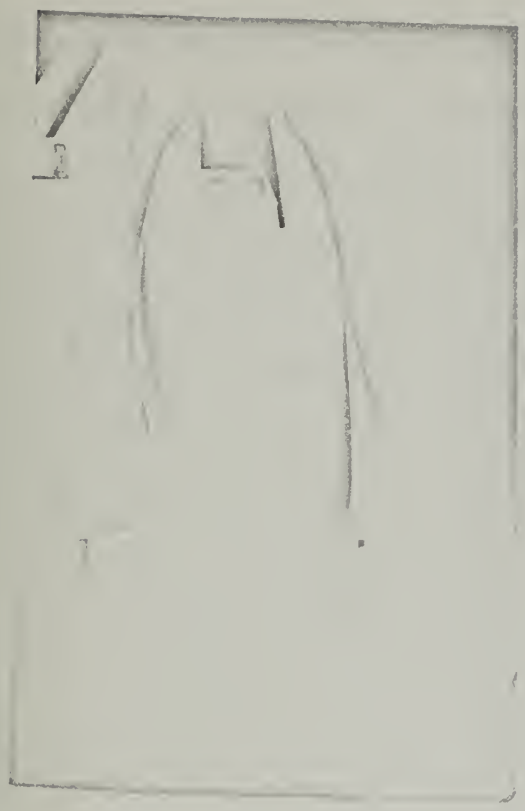

experimental results which have been published to date. Chapter III presents the theory used in organizing this work. Chapter IV describes the equipment used including the model, the tank, the force detectors and the pressure detectors. In addition it details the way in which each piece of equipment was used and the analytic procedures used to obtain the results. Chapter V presents the detailed results of the work in graphical or tabular form. Chapter VI draws upon the results of the preceding section and presents the conclusions that were reached concerning the results themselves and the experimental procedure used in obtaining them. Chapter VII gives some potential applications of the two-phase propulsion system and gives a listing of some of the engineering considerations and problems which might arise from use of this propulsor. This section also provides someone interested in further work on the two-phase propulsor with some ideas about what has not yet been investigated but deserves further consideration.

Appendix A is provided for reader convenience and simply details Kostilainen's momentum balance and energy balance calculations. Appendix B shows the details of calculating C_{ϕ}, C_{TS} and η (the principle parameters used in describing the phenomenon under investigation) for one operating condition.

Tables in this thesis provide the averaged data from the experiments so that it will be available to future researchers that wish to adopt a different analysis approach to the problem than the one followed by the author.

II. STATE OF THE ART

A. Theoretical

As noted in the Introduction, Professor Kostilainen of the Finland Institute of Technology has been studying the two-phase propulsion system. He has completed a dimensional analysis and solved a momentum balance and an energy balance on an idealized model of the system. The details of his calculations can be found in Appendix A, but the results are summarized below. The notation in the equations below is not Kostilainen's original notation but rather that of the author. The change in notation was prompted by the fact that Kostilainen has used some symbols which have very specific meaning to naval architects and stand for different quantities. For example he calls B the breadth of the channel, but B is most commonly used to denote ship's beam.

Kostilainen's dimensional analysis results in the following three equations.

$$C_{TS} = \frac{T}{\rho g B_c h^2}$$

$$\phi_K = \frac{V_G}{B_c h \sqrt{gh}}$$

$$F_{nh} = \frac{U_L}{\sqrt{gh}}$$

where: C_T = Thrust coefficient

T = Thrust created by the two-phase propulsion system, parallel to the ship's fore and aft axis

ρ = Mass density of water

g = Acceleration due to gravity

B_c = Width of the channel

h = Depth of the orifices

ϕ_K = Air flow rate coefficient

V_G = Volumetric air flow rate

F_{nh} = Froude number (modified)

U_L = Velocity of the liquid at the orifices

Unfortunately the results of his momentum balance include quantities which cannot be measured, such as the amount of water that gets accelerated and the final velocity of the water leaving the ramp, and are therefore not very useful to an experimenter. He does however show that the propulsor efficiency, η, is

$$\eta = \frac{TU_L}{\rho V_G g h} \quad .$$

B. Experimental

Published information from Kostilainen to date describes two geosim models with a scale factor of 4 and the results of his self propelled tests. Because he decided not to measure the thrust of the two-phase propulsor he was obliged to find another way of presenting his data, and he therefore defined an "apparent thrust," T_A, which is the force required to tow the model at a prespecified speed without any air flow, henceforth referred to as the bare hull drag, minus the force required "tow" the model at the same speed with the propulsor in operation. It should be pointed out that the apparent thrust includes not only the real propulsor thrust but also any changes in the actual hull resistance which result from changes in the flow pattern and pressure distributions caused by the presence of the air in the channel. The apparent thrust coefficient then is

$$C_{TA} = \frac{T_A}{\rho g B_c h} \quad .$$

Kostilainen found, using the above dimensionless coefficient, that for low air flow rates, i.e., $\phi_K \leq .2$, the bollard pull tests, i.e., tests with model velocity of zero, the results were independent of model size and at higher flow rates the bollard pull test results showed weak dependence on model size. The dependence on model size increased with Froude number and at the self propelled point was large enough so that correlation was almost nonexistent.

Some very important results of Kostilainen's work are that the model velocity, U, is a fair approximation to U_L, the liquid velocity at the orifices, and that the thrust is mainly dependent upon the Froude number

and the air flow rate.

III. THEORY

When ship propulsion is being considered at least three quantities are of interest; thrust from the propulsor, its efficiency and resistance of the hull. Hull resistance for a normal displacement vessel is known to be fairly well predictable by Froude's hypothesis and it is mostly a function of the Froude number and the Reynolds number.

For a two-phase propulsor driven ship it is postulated that the hull resistance is a function of the dimensionless air flow rate, the Froude number, F, and the Reynolds number, R, i.e.,

$$C_T = \tfrac{1}{2}\rho S U^2 f\left(\frac{V_G}{L^2\sqrt{gL}}, \frac{U}{\sqrt{gL}}, \frac{UL}{\nu}\right)$$

where

C_T = total resistance coefficient

ρ = density

S = wetted surface of the ship

U = speed of the ship

V_G = velumetric air flow rate

g = gravitational constant

L = length of ship

ν = viscosity of water

It is additionally hypothesized that:

$$\frac{C_T}{\tfrac{1}{2}\rho S U^2} = C_R\left\{\frac{U}{\sqrt{gL}}\right\} + C_F\left\{\frac{UL}{\nu}\right\} + C_\phi\left\{\frac{V_G}{L^2\sqrt{gL}}, \frac{U}{\sqrt{gL}}\right\}$$

where

C_R = residuary resistance coefficient

C_F = frictional resistance coefficient

C_ϕ = air flow resistance coefficient

ϕ is now defined as

$$\phi = \frac{V_G}{L^2\sqrt{gL}}$$

C_R plus C_F is interpreted as the bare hull resistance, i.e., the resistance with no air flowing in the channel. Having made this final postulate, the resistance equation can be interpreted as saying that the bare hull resistance, C_{BH}, plus the air flow resistance equals the total resistance, i.e.,

$$C_\phi = C_T - C_{BH}$$

If all of the above is correct, then a knowledge of C_ϕ as a function of the dimensionless air flow rate and the Froude number will allow prediction of the full scale ship resistance from the model resistance.

Knowledge of C_T alone is not sufficient information to do a powering calculation for the two-phase propulsion system. Two options will be presented in this thesis for obtaining the power requirements of a full sized ship.

The first option is to try Kostilainen's nondimensionalizing coefficients on the thrust (not the apparent thrust as he did). Therefore a new thrust coefficient, C_{TS}, is defined as

$$C_{TS} = \frac{T}{\rho g B_c h^2} \quad .$$

Since it does not contain the change in hull resistance caused by air in the channel as C_{TA} did in Kostilainen's work, it may correlate better than C_{TA} did.

Under this first option then, C_ϕ and C_{TS} are presumed to be known for the model and they are of course both functions of ϕ and Γ. Along with knowledge of C_ϕ and C_{TS} it is assumed that the C_{BH} has also been measured for the model so that C_Γ and C_R are known. To obtain the powering requirements for a full sized ship with a known scaling factor and at a specified speed the following procedure could be used.

The scaling factor and the speed can be used to calculate R and Γ which can be used to obtain C_Γ and C_R for full scale, thus providing C_{BH} full scale. Entering the C_ϕ curves with the given Γ provides C_ϕ values for various values of ϕ. These values of C_ϕ are added to C_{BH} to give C_T from which the total hull resistance can be obtained and then plotted as a function of ϕ. Now C_{TS} can be obtained from its curves as a function of ϕ, and, since $\rho g B_c h^2$ for the full sized ship is known, the thrust can be calculated and plotted on the same graph as the resistance was plotted. Where the curves cross the thrust equals the resistance and the ship is self propelled. The crossover point also determines ϕ and therefore the input power requirement can be calculated since

Power Input = $V_G \rho g h$.

The second option is that of recognizing that the efficiency, η, is a nondimensional number and may be a useful tool in extrapolating from the model to full scale. Since the power input and output can be calculated from measurable quantities on the model, it may be possible to establish a family of curves of η as a function of ϕ and Γ.

$$\eta = \frac{TU}{V_G \rho g h}$$

So for this option it is presumed that C_ϕ and η are known as a function of

ϕ and F. To obtain the powering requirements for a full sized ship with a known scaling factor and at a specific speed the following procedure could be used.

The total hull resistance can be obtained as it was in the preceding option and plotted against ϕ. The thrust can be calculated for the full scale by entering the family of η curves with the specified F and thereby obtaining η as a function of ϕ. Utilizing that knowledge and the equation above for η it is possible to calculate T for specific values of ϕ and then plot them on the resistance plot. At the crossover point the resistance equals the thrust and the ship would be self propelled. ϕ would then be known at the self propelled point and the input power requirement calculated.

IV. EXPERIMENTAL PROCEDURE

A. Equipment

Two geosim models were built on a scale factor of 1.5 having L = 4.5 feet and 6.75 feet. Figure 2 is a lines drawing of the geometric configuration used. Table 1 lists the major dimensional characteristics of the two models. Δ is defined as the vertical height of the air chamber. δ is the inner diameter of the air supply pipe to the air chamber. The models were made of six pound per cubic foot urethane resin insulation which was cut and molded to shape and then sealed with three coats of fiberglas finishing resin. Each coat of resin was sanded to a smooth finish. Two coats of spray epoxy paint were then used to finish the surface. Turbulence pins were glued to the models at both stations 2 and 4 on a 1/2" and 3/4" spacing between pins for the small and large model respectively. The force detector mounting platforms were located with their midpoints at station 8 on the waterline. Lead ballast was used to give each model its proper displacement and zero trim.

The models were towed in the Massachusetts Institute of Technology Ship Model Towing Tank. The tank width is 102 inches and the water depth was 42 inches. The carriage travel had a programed acceleration followed by 150 foot travel at uniform speed and then a programed deceleration. Speeds are accurate to within 1%. Over the period of time the tests were conducted the fresh water in the tank did not vary over one degree from 78° F. All calculations have been based on that temperature.

Two different force detectors, a torque meter and a force block, were used because the torque meter could not tolerate the large acceleration forces that were experienced during the acceleration and deceleration

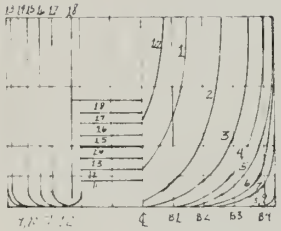

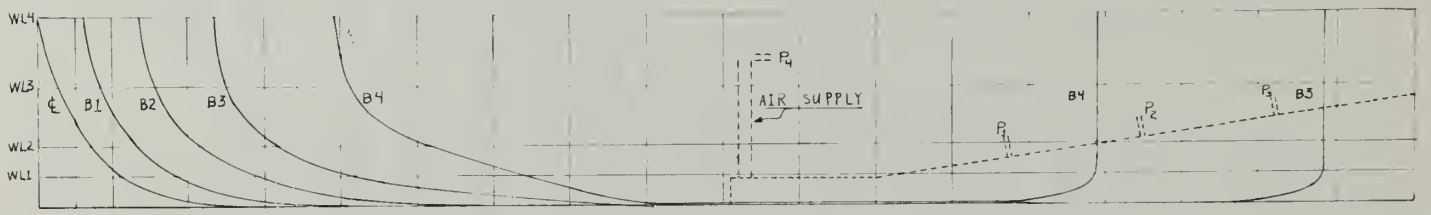
WL4
WL3
WL2
WL1
℄
B1
B2
B3
B4
P4
AIR SUPPLY
P1
P2
P3

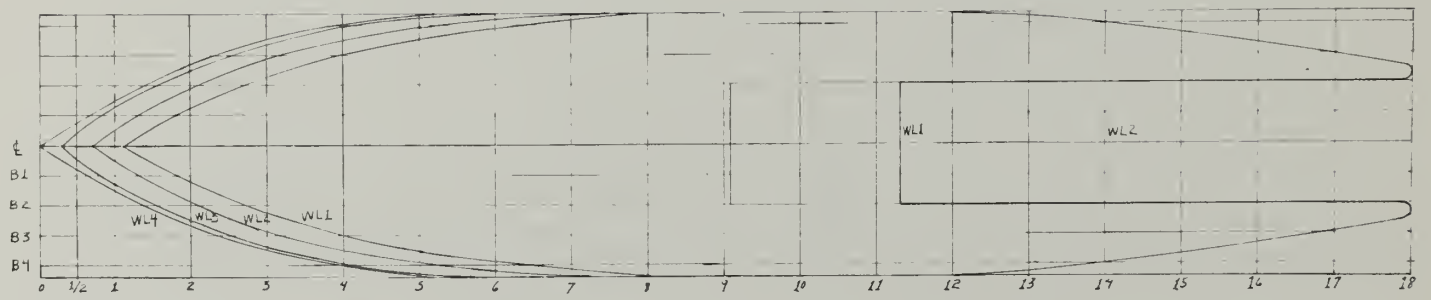
℄
B1
B2
B3
B4
WL4
WL3
WL2
WL1
0
1/2
1
2
3
4
5
6
7
8
9
10
11
12
13
14
15
16
17
18

TABLE 1.

MODEL PARAMETERS

Symbol	Description	Model A	Model B
L	Length	4.5 ft.	6.75 ft.
B	Breadth	10.5 in.	15.75 in.
B_c	Breadth of channel	4.875 in.	7.31 in.
S	Wetted surface area	7.76 sq. ft.	17.50 sq.ft.
Δ	Vertical height of air chamber	1.0 in.	1.5 in.
β	Angle of ramp to water surface	12.4°	12.4°
δ	Inner diameter of the air supply pipe	0.5 in.	.75 in.
C_p	Prismatic Coefficient	.996	.996
h	Depth of orifice	5.625 in.	8.44 in.
∇	Displacement	75.3#	254.3#

of the carriage when the large model was being towed, but it gave greater accuracy for measuring the smaller forces associated with the smaller model. Both meters were calibrated several times during their use and each was determined to be linear to within 1% to forces of 1.5 lbf and 3 lbf for the torque meter and force block respectively.

The torque meter was a variable resistance balanced bridge type while the force block was a variable reluctance detector. Both were connected to a transducer with a D.C. voltage output which was battery biased with a 5 vdc battery. The biasing was used to keep oscillations in the D.C. level from passing through zero thereby causing malfunction of the voltage to frequency converter which was used to feed a pulse counter that was automatically started by the carriage after it had reached uniform speed.

The model was further instrumented with four pressure taps feeding pressure transducers. The taps, P_1, P_2, P_3, were located at three equally spaced points on the channel ramp so that P_1 was nearest the air chamber and P_3 was nearest the stern and they divided the ramp into four equal sections. The fourth tap, P_4, was installed in the air supply piping just above the air chamber. The pressure transducers had a 1% accuracy over the range 0 to .5 psi. They were of the variable reluctance balanced bridge type used with carrier preamplifiers which provided resistance and capacitance balance plus rectification of the output signal. The output was recorded on a multichannel chart recorder. The pressure recording system was calibrated several times during the course of the experimentation using a manometer and a static head of up to ten inches of water.

Air was supplied to the model from 130 psi air system on the carriage.

A pressure reducer was used to control the pressure at the inlet to the rotometer used for measuring the air flow. The air flow rate was set by means of a needle valve. The rotometers were of the gravitational floating ball type and had maximum flow rates of 92 cfh and 1482 cfh. The air supply could provide only about 700 cfh without significant loss of pressure and therefore loss of accuracy of measurement.

B. Operational Procedure

The operational procedure, i.e., those functions which were performed to obtain the data, were for all practical purposes the same for both models.

The first requirements were those of calibration. The force detector, after being connected to the transducer, the battery, the voltage to frequency converter and the counter, was calibrated by using a one-pound weight to supply the force. Both force detectors were also checked for linearity by using various weights over the ranges of interest. Both detectors were linear to within ±1%.

The pressure transducers also required calibration. They were all connected to a water manometer and their output measured on the recorder, after resistive and capacitive balancing had been accomplished on the electrical system. The manometer readings were plotted against the recorder readings for various pressures from one to ten inches of water to check linearity and for accurate calibration. The recorded outputs were linear to within ±5%.

Each model was attached to its appropriate force detector, which was attached to the carriage. The model had freedom of motion in both pitch and heave but was restrained in yaw by the force detector. After the model was attached to the carriage the air supply flexible piping and the pressure taps flexible connections were made and sealed using rubber sealant. The transducers were again balanced both resistively and capacitively and the static pressure was nulled out by using bias on the preamp so that the detector measured the deviation from the static condition.

Bare hull resistance runs, i.e., without any air flowing, were then

made and the force, speed and pressure distribution measured. Each run consisted of running the model the length of the tank at uniform velocity (exclusive of acceleration and decelerations at the beginning and end of each run). Several runs were made for each speed.

Bollard pull tests were conducted with the carriage stopped, i.e., zero velocity, and the air flowing at some desired rate. The air flow rate was measured with the rotometer and the force and pressure distribution were measured as in the bare hull resistance runs.

If the air flow rate changed over the run by more than 2% the run was performed over again. The bollard pull test was conducted several times on each model so that the average results could be used with confidence of repeatability.

Finally, runs which henceforth will be called the self-propelled model tests, were conducted near the self-propelled point and the force, velocity and air flow rate were measured and the pressure distribution was recorded. The procedure was to start the air flowing and adjust it to the desired rate with the model stopped. The model was then accelerated to speed and the force on the detector measured and the pressure distribution recorded. After the model was stopped the air flow rate was again measured and if the rate had changed by more than 2% the run was conducted again. Several runs were made at each velocity-air flow rate combination.

After the self-propelled tests had been completed at a given velocity, the bare hull resistance was measured again at that velocity.

C. Analytical Procedure

(1) Bare Hull Resistance Coefficients.

The first calculations to be made were those which established that the models operating without air obeyed Froude's hypothesis in spite of the presence of the ramp in the aft section of the ship.

$$C_T = C_R + C_F = \frac{D_T}{\frac{1}{2}\rho S U^2}$$

where D_T = total resistance (measured).

Reynolds number and Froude number were calculated for both models at 78° F. Knowledge of Reynolds number provided the required input for calculating C_F in accordance with the formula for the ITTC line[4]

$$C_F = 0.075/(\log_{10} R - 2)^2$$

The average of several runs at the same speed was used to increase the accuracy of D_T and C_T was then easily calculated. C_R was simply then the difference between C_T and C_F. For the model with L = 4.5 ft. C_R could be used after the above calculation was complete but for the longer model, L = 6.75 ft., a correction had to be made because the model was large enough so that the model-wall and bottom interaction force was large enough to affect the resistance coefficient. This interaction force, after being nondimensionalized by division by $\frac{1}{2}\rho S U^2$, is called the tank blockage coefficient, C_B.

Scott[5] has presented a way for calculating C_B based on the tank dimensions, the model displacement and dimensions and the Reynolds number. These numbers have been presented in Table 3. Their inclusion in the above calculation then resulted in values of C_R for the large model (L = 6.75 ft.). C_R is plotted and discussed in the next chapter.

(2) Bollard Pull Tests

The next calculation that needed to be made was the bollard pull calculation which is actually two separate calculations. One part of the calculation is very trivial and simply required that the forces as measured by the force detector be averaged over the runs that were made at a given air flow rate. This force could then be nondimensionalized by division by the factor $\rho g B_c h^2$ if desired to yield C_{TS}.

The second part of the bollard pull test was more complicated to perform but the idea behind it was quite simple. The pressure distribution on the ramp and the front of the air chamber, called the step, was to be integrated to give the total force created by the two-phase air-water mixture.

The pressures at the center of the channel had been recorded on charts and therefore had to be first converted from chart dimensions to pressures using the various calibration factors that had been measured. The pressures were then averaged over all the runs which had the same air flow rate. It was assumed that the pressure distribution was not a function of the athwartships position. Plots of these pressures are in the results section, Figures 6 and 7. The area under each curve is proportional to the force on the ramp and therefore each curve was integrated using Simpson's first rule.[4] The force on the ramp is equal to the sine of the ramp angle times the width of the channel times the integral of the pressure distribution curve (which has units of pressure times distance).

The above integrated force, F_I, does not account for the force created by the over pressure in the air chamber acting against the step. This force is called the step correction force, Step Corr. The over

pressure in the air chamber is P_4 but it does not act against the full area of the step, only an area which is equal to the width of the step (channel width) times the over pressure in inches. The idea here is that the over pressure, P_4, in the chamber is on the average equal to the vertical height of the layer of air in the chamber since P_4 equal to zero implies a static pressure of $h - \Delta$ inches of water. One indication that this is a more reasonable approach to the calculation of the step correction force than that of using the full step area is that calculations made using the full area resulted in calculated forces greater than the measured forces.

By adding the ramp force and the step correction force together the total force created by the two-phase propulsor could be obtained, T. This force was used in both a dimensional and nondimensional form. See Figures 8 and 9.

(3) Ramp Drag

The ramp drag or bare hull ramp drag, R_D, is a name that has been given to the final results of the calculation which is described below. Essentially it is the sum of the Step Corr and the integrated force on the ramp when the model is moving but no air is flowing. It has no real physical meaning and is simply used as a tool to achieve a result.

(4) Thrust Provided by the Two-Phase Propulsion System

A look ahead at the thrust calculation in Section IV.C.5 will disclose that under many velocity-air flow rate combinations the pressures are mostly negative and that the result of the integration is negative yet

there has been a decrease in the measured force required to move the hull at that speed compared to the bare hull runs. The point is that the integrated pressure on the ramp is less negative with air than without and the net difference is the thrust on the ramp provided by the two-phase propulsion system. This thrust could have been calculated by taking the pressure distribution with air and subtracting the pressure distribution without air from it and then performing an integration procedure like the one detailed in the preceding section for the bollard pull tests. However, since the integration is linear in pressure and distance the two pressure distributions can be done separately and the results subtracted to yield the same answer.

(5) Self-Propelled Model Tests

Self-propelled model tests are to provide three additional pieces of information; the self-propelled speed as a function of the air flow rate, the resistance of the hull with air flowing, and the thrust from the two-phase propulsion system.

The analytic procedure required to get the self-propelled speed as a function of the air flow rate could have been as simple as plotting the counts measured by the counter measuring force against the air flow rate and then establishing the constant velocity lines. When the counts passed through zero (i.e., at zero force) the model had to have been self propelled at that air flow rate and velocity. To make the graphs more meaningful the counts were changed to forces. For accuracy the results of many runs for each velocity-air flow rate combination were averaged and then plotted.

To present the data in a more easily assimilated form, the self-

propelled velocities and air flow rate combinations for each model was nondimensionalized to F and ϕ and plotted together. (See Figure 15.) These numbers will be needed later to locate the self propelled points on other curves.

The Force, T_m, measured by the force detector when the model is moving with the air flowing when subtracted from the thrust developed by the propulsor yields the second desired result, i.e., the resistance of the hull, D_T. T_m and D_T can be nondimensionalized as needed. (Note that when the air is providing more thrust than is needed to overcome the resistance of the hull that the measured force T_m is positive.)

The thrust provided by the two-phase propulsion system is to be obtained by integrating the pressure distribution. The pressures were recorded on chart paper. Calibration numbers were used to change the chart dimensions to inches of water and the pressures were then averaged over runs with almost the same air flow rate and velocity. These pressure distributions were then handled in the same manner as the bollard pull tests were with one exception. To obtain the thrust it is necessary to subtract the ramp drag from the integrated force on the ramp and the step correction force. The resultant is the total thrust created by the two-phase propulsion system along the ship's fore and aft axis, T.

The final few calculations to obtain $C_\phi(F, \phi)$, $\eta(F, \phi)$ and $C_{TS}(F, \phi)$ are simply obtainable from the thrust by arithmetic.

$$C_\phi = \frac{T}{\frac{1}{2}\rho S U^2} - C_{BH}$$

All of the numbers are known and C_{BH} has already been calculated as part of the procedure of IV.C.1, the calculation of C_R to prove Froude scaling.

η is calculated using

$$\eta = \frac{TU}{\rho g V_G h}$$

since the value of all of the terms has been established. C_{TS} is obtained from the thrust using the nondimensionalizing coefficient $1/\rho g B_c h^2$.

V. EXPERIMENTAL RESULTS

A. Establishment of Froude Scaling of the Models

Both models were towed in the tank over as wide a range of speeds as the tank equipment and models could permit. Though the steady state forces were generally less than two pounds force, the inertial acceleration forces on the carriage and the force block or the torque meter were large enough to cause concern for those pieces of equipment and thereby limited the range of speeds available for testing.

Below a Froude number of 0.08 the scatter in data was unacceptably high and therefore the data are not presented. The scatter was caused by random transition from laminar to turbulent flow under conditions which were such that the frictional contribution to the model's resistance was greater than 50%.

Figure 3 shows the residuary resistance coefficient plotted as a function of the Froude number. The total C_T, C_F and the blockage correction[5] coefficient if applicable are tabulated in Tables 2 and 3. C_R is never the dominant contributor to C_T and therefore the magnitude of C_R is very sensitive to the fractional contribution the experimenter postulates. The ITTC line was used in that calculation because the history of the towing tank indicates that has been the most successful estimation of C_F and given the best correlation with larger models, full sized ships and models run at other tanks.

Without the blockage correction for the 6.75 ft. model the correlation would be very poor. With it, however, the models are seen to be basically similar above a Froude number of about 0.15. Below that value

Figure 3

Residuary Resistance Coefficient, C_R,

vs Froude Number, F

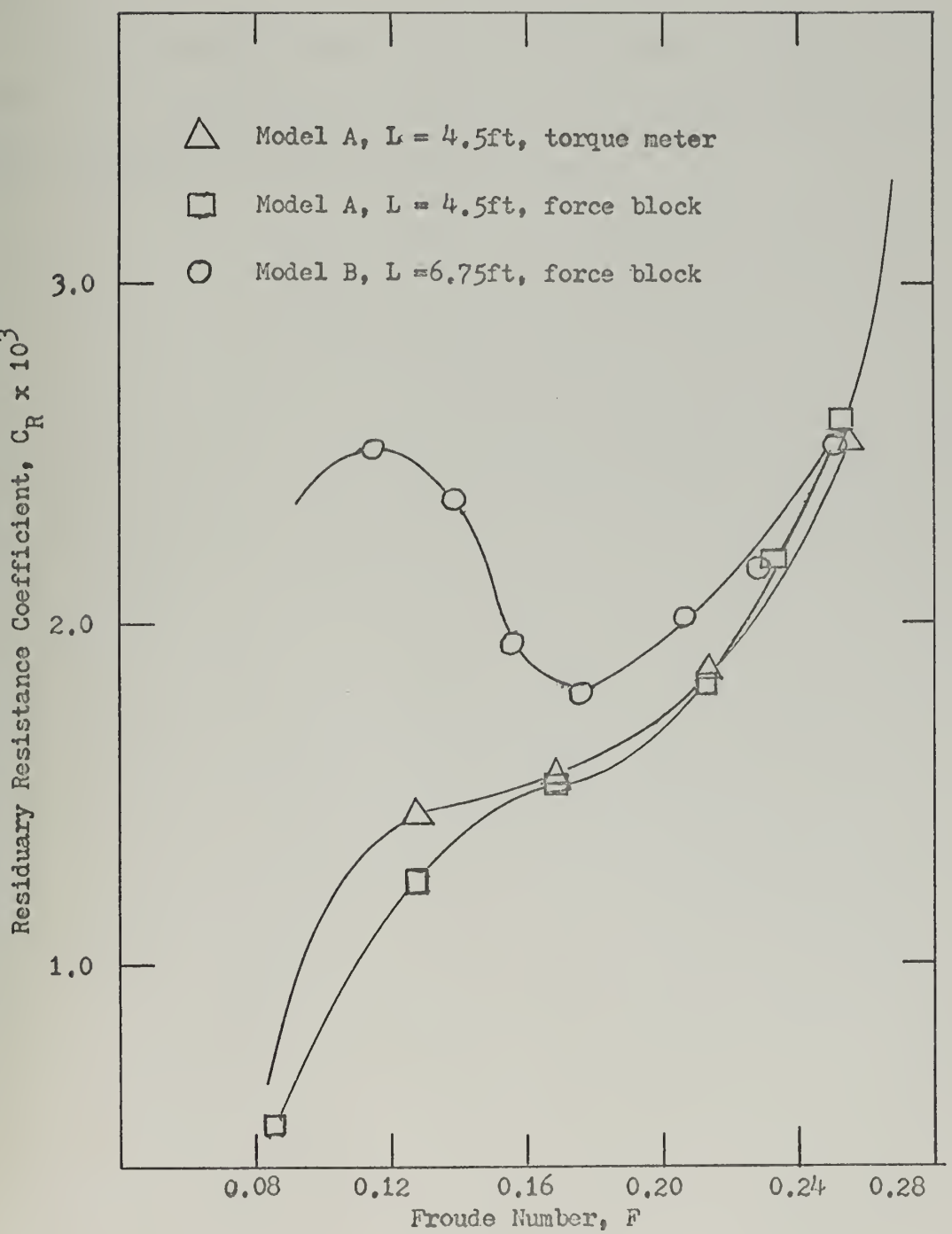

the 4.5 ft. model is in the transition zone of the fractional contribution while the 6.75 ft. model is still well above that zone. This causes the calculation procedure to artificially depress the C_R curve of the smaller model.

Also plotted in Figure 3 is the 4.5 ft. model as measured with the force block, and this plot is presented as verification that the two force measuring devices yield similar results.

Table 2

Bare Hull Resistance
Model A

Model L = 4.5 ft

Speed KTS	Froude Number	Reynolds Number ($x10^5$)	C_T	C_F ITTC	C_R
.310	.0435	2.48	.0051	.00651	-.0014
.610	.0855	4.88	.0054	.00551	-.0002
.901	.1268	7.22	.00649	.00504	.00145
1.201	.1686	9.61	.00629	.00473	.00156
1.510	.2118	12.10	.00636	.00450	.00186
1.802	.2525	14.43	.00684	.00433	.00251
2.013	.2823	16.12	.00904	.00424	.00480

Table 3

Bare Hull Resistance
Model B

Model L = 6.75ft

Speed KTS	Froude Number	Reynolds Number ($x10^5$)	C_T	C_F ITTC	C_R (Uncorrected)	C_B	C_R
.839	.0960	10.1	.00777	--	--	--	--
1.006	.1151	12.1	.00719	.00450	.00269	.00018	.00251
1.201	.1377	14.5	.00684	.00433	.00251	.00014	.00237
1.351	.1548	16.2	.00629	.00423	.00206	.00013	.00193
1.510	.1730	18.2	.00620	.00413	.00207	.00015	.00192
1.645	.1885	19.8	.00600	.00406	.00194	.00015	.00179
1.802	.2064	21.7	.00618	.00399	.00219	.00017	.00202
1.985	.2275	23.9	.00625	.00391	.00234	.00018	.00216
2.194	.2515	26.4	.00659	.00383	.00276	.00024	.00252
2.233	.2559	26.8	.00687	--	--	--	--

B. Bollard Pull Tests

The bollard pull test is of interest for two reasons. It establishes the zero velocity value of the thrust. In addition to that needed function it can also be used as a source of information concerning errors for the forces calculated from pressure-area integrations. The bollard pull force and the bollard pull pressure distribution were measured simultaneously and therefore the error introduced by the integration process can be evaluated by comparison of the measured and calculated values.

Figures 4 and 5 show the pressure distribution of these two tests. Nondimensional plotting of these quantities using the factors that are used elsewhere in this thesis does not cause the dissimilarities to disappear. The most noteworthy dissimilarity is that P_4 is always the highest pressure on the 6.75 ft. model, and this is not the case on the 4.5 ft. model. The second most important change is that P_3 and P_1 have changed positions. Since P_1 is the closest measurement point to P_4 it is surprising that P_1 is highest with the lowest being P_4. These differences imply that the flow patterns of the two models are different. In order to obtain a little more insight before we try to determine the consequences of the above implication the pressures were plotted against their position on the ramp. Again the dissimilarities are easily spotted, even though the overall shapes are comparable.

One of the basic assumptions that has been made in attempting to understand the two-phase propulsion system is that some form of nondimensionalization can be used to make the hulls "similar" on the basis of force scaling. It is expected that, even though the flow patterns are dissimilar, the forces of interest can be scaled by the use of the proper procedure.

Figure 4

Bollard Pull Test Pressure Distribution as a

Function of the Air Flow Rate for Model A

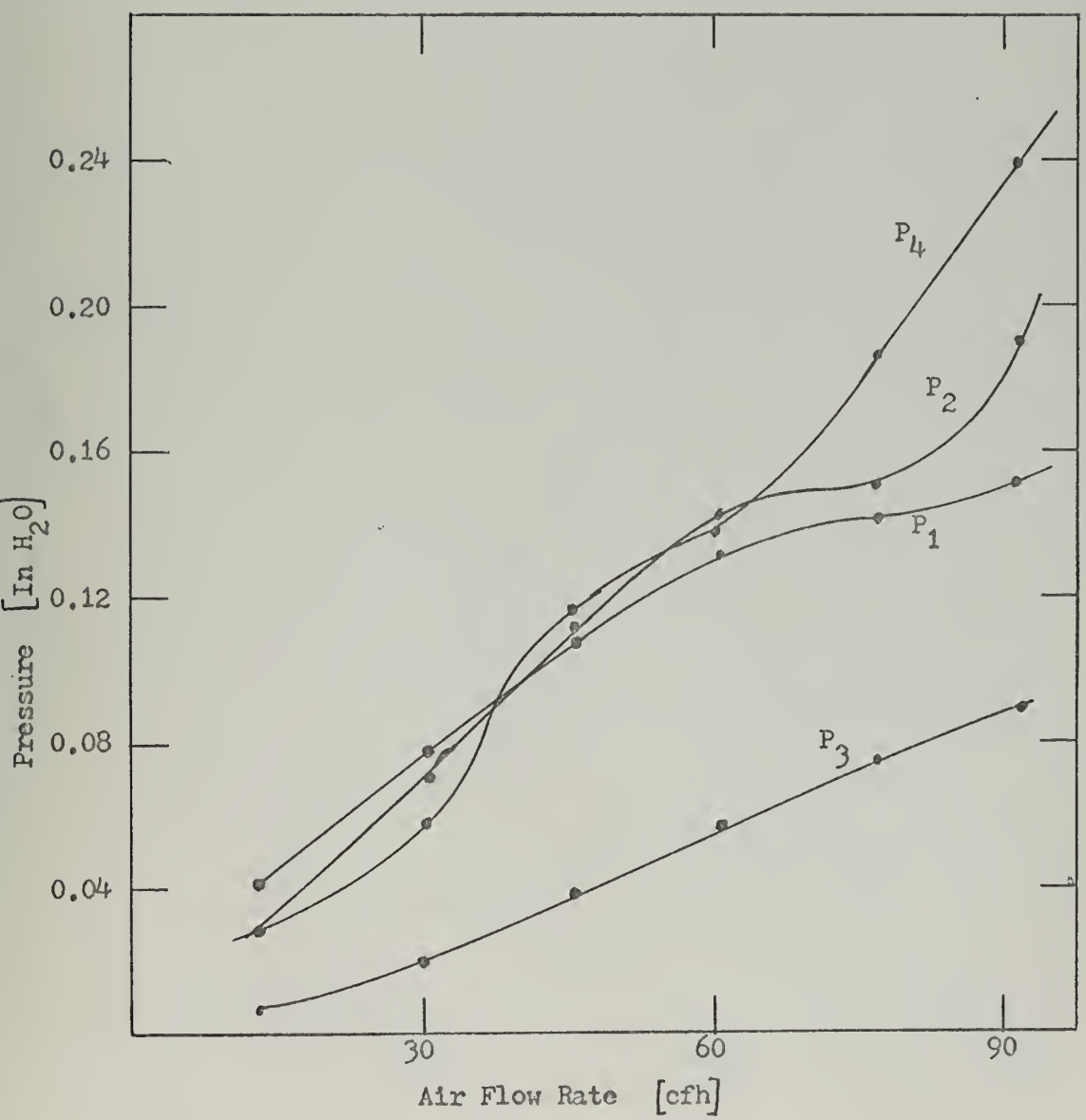

Figure 5

Bollard Pull Test Pressure Dristribution as a

Function of the Air Flow Rate for Model B

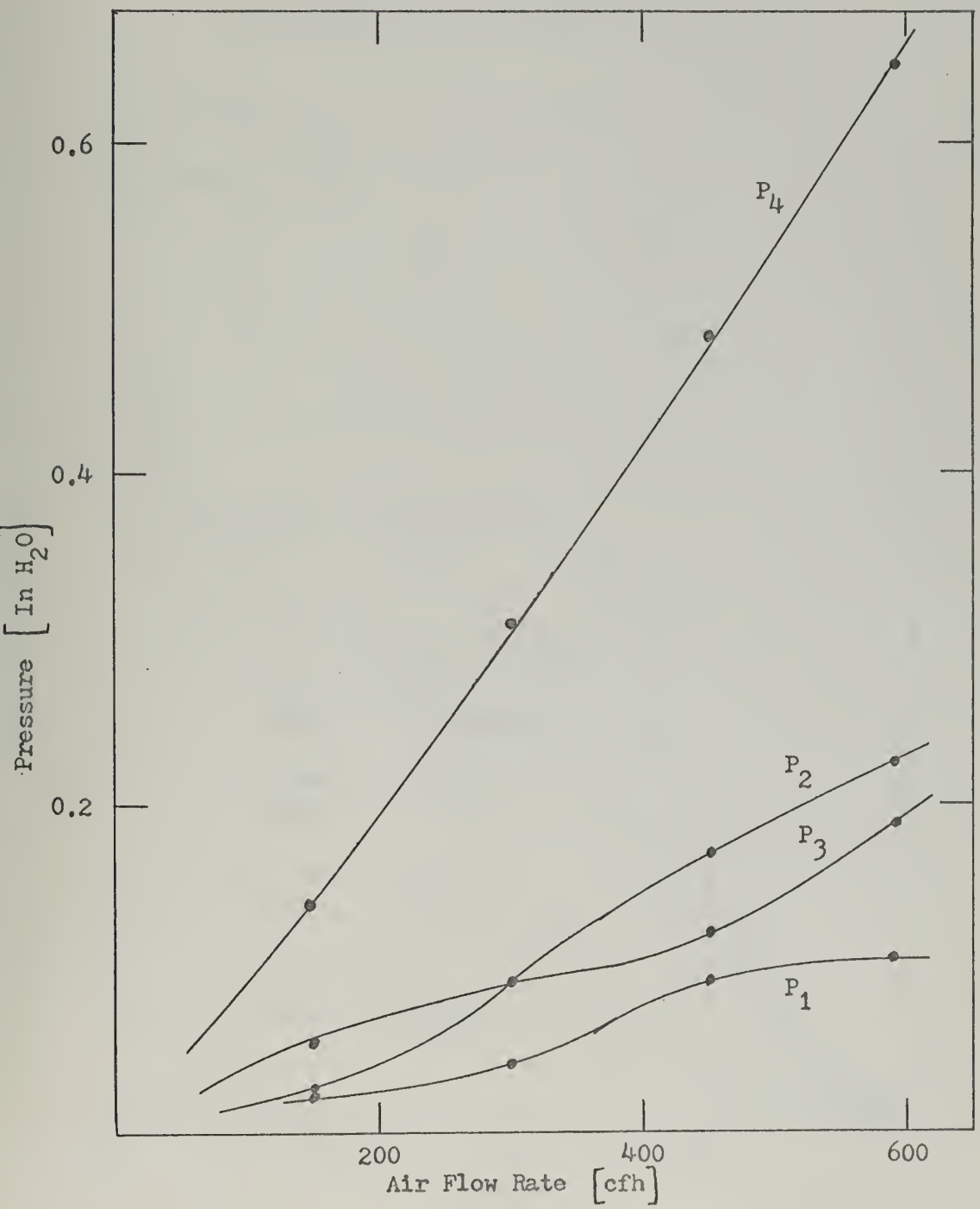

Figure 6

Bollard Pull Test Pressure Distribution

as a Function of Position for Model A

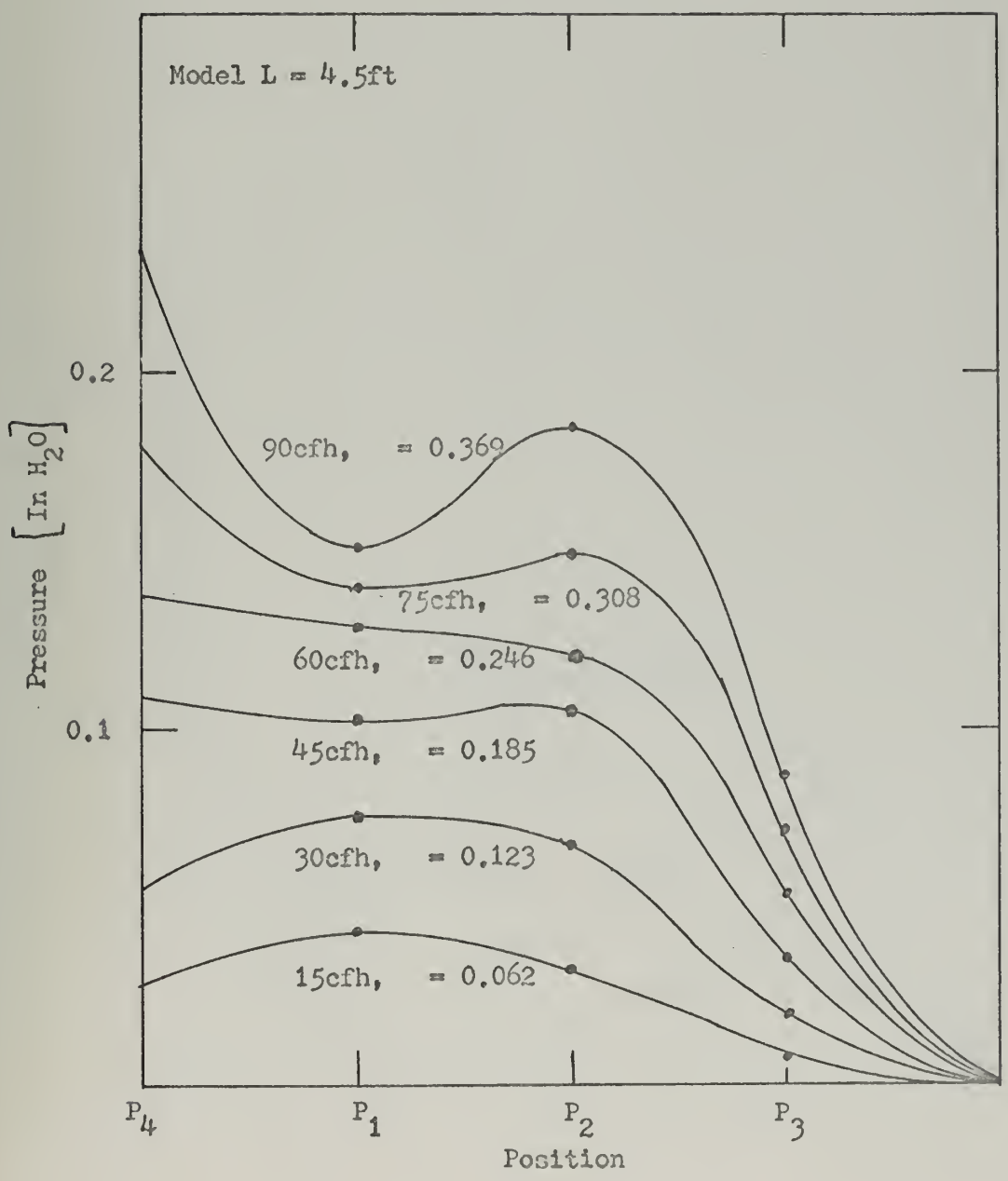

Figure 7

Bollard Pull Test Pressure Distribution

as a Function of Position for Model B

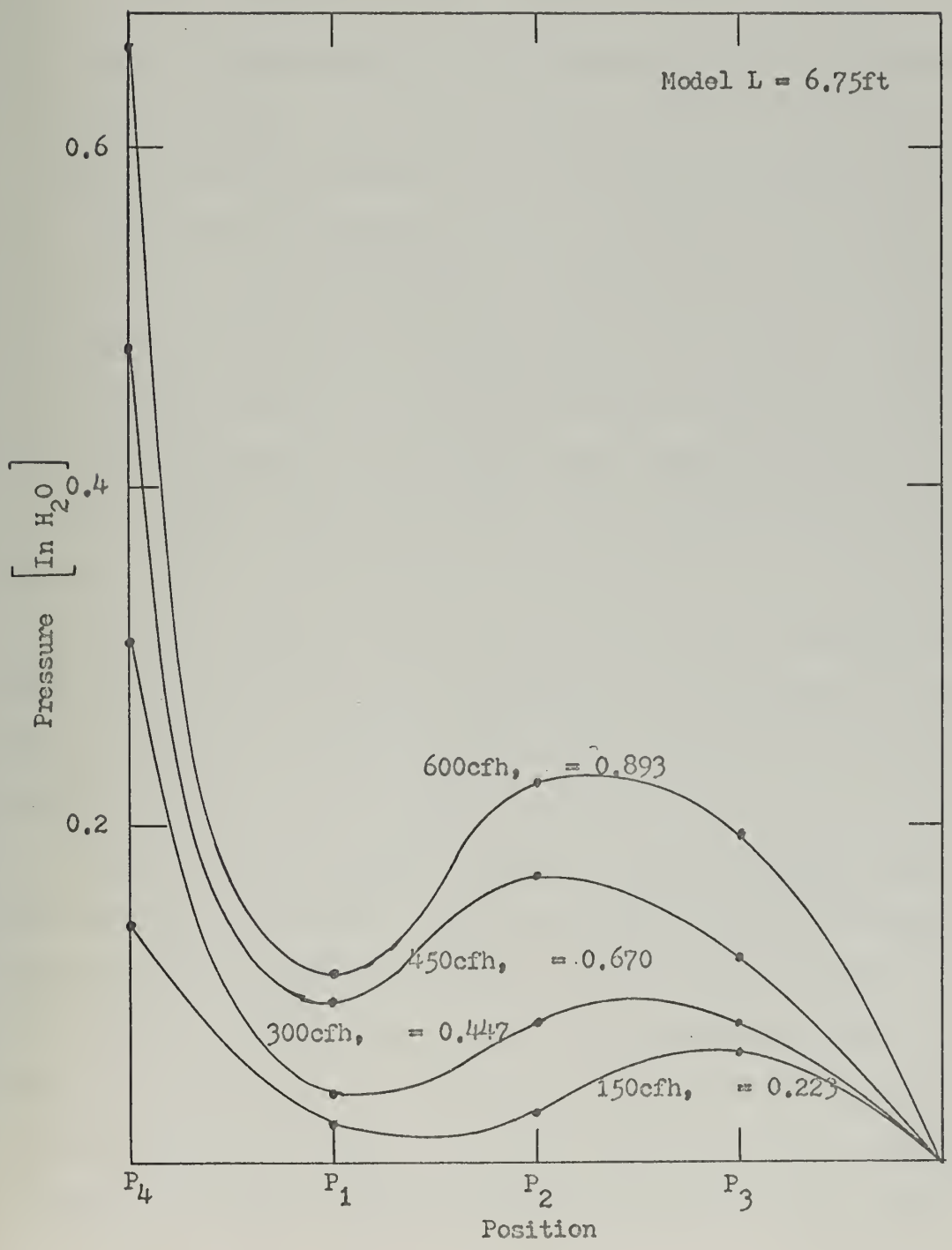

This hopeful expectation is based on the successful application of Froude's hypothesis.

One plausible explanation of the dissimilarities is that frictional forces are more predominant in the smaller (L = 4.5 ft.) model. Kostilainen has postulated that this is the case and this work seems to verify that postulate. The reason for believing this is that the increase in dynamic pressure is shifted in the direction of the source on the small model, thus indicating that the air-water mixture has been obliged to do more work, i.e., has lost more energy over the first portion of its travel. This also implies that it has proportionally worked against a larger force. This correlates with the fact that on the smaller model the local Reynolds number for the position of each of the three probes on the ramp is smaller than for the large model which implies that frictional forces will be more dominant.

One conclusion that can be drawn now is that any nondimensionalizing scheme which does not treat the frictional forces separately will probably not be successful at scaling the total thrust produced by the two-phase propulsion system.

Figures 8 and 9 show the comparison of the calculated forces to the measured forces in each case. The steps which lead from the pressure distribution to the integrated force value are tabulated in Tables 4 and 5 . Both integrals yield low values. They are not proportion errors. One apparently is in error by a fixed additive value, while the other if off by a fixed multiplicative value. At least a part of the error is probably the result of assuming that the pressure distribution is flat across the

Figure 8

Bollard Pull Test Calculated and Measured Forces

as a Function of Air Flow Rate for Model A

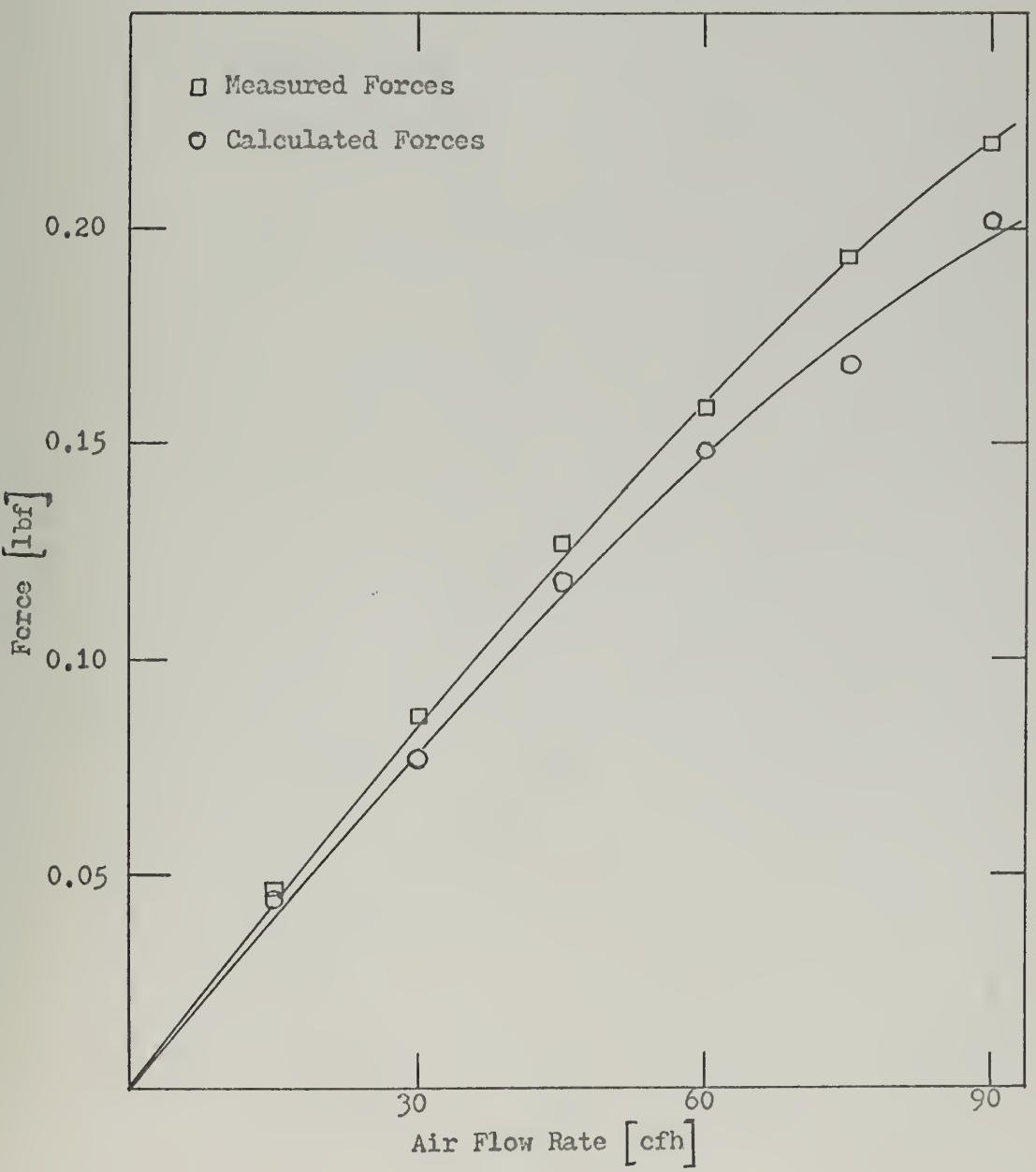

Figure 9

Bollard Pull Test Calculated and Measured Forces

as a Function of Air Flow Rate for Model B

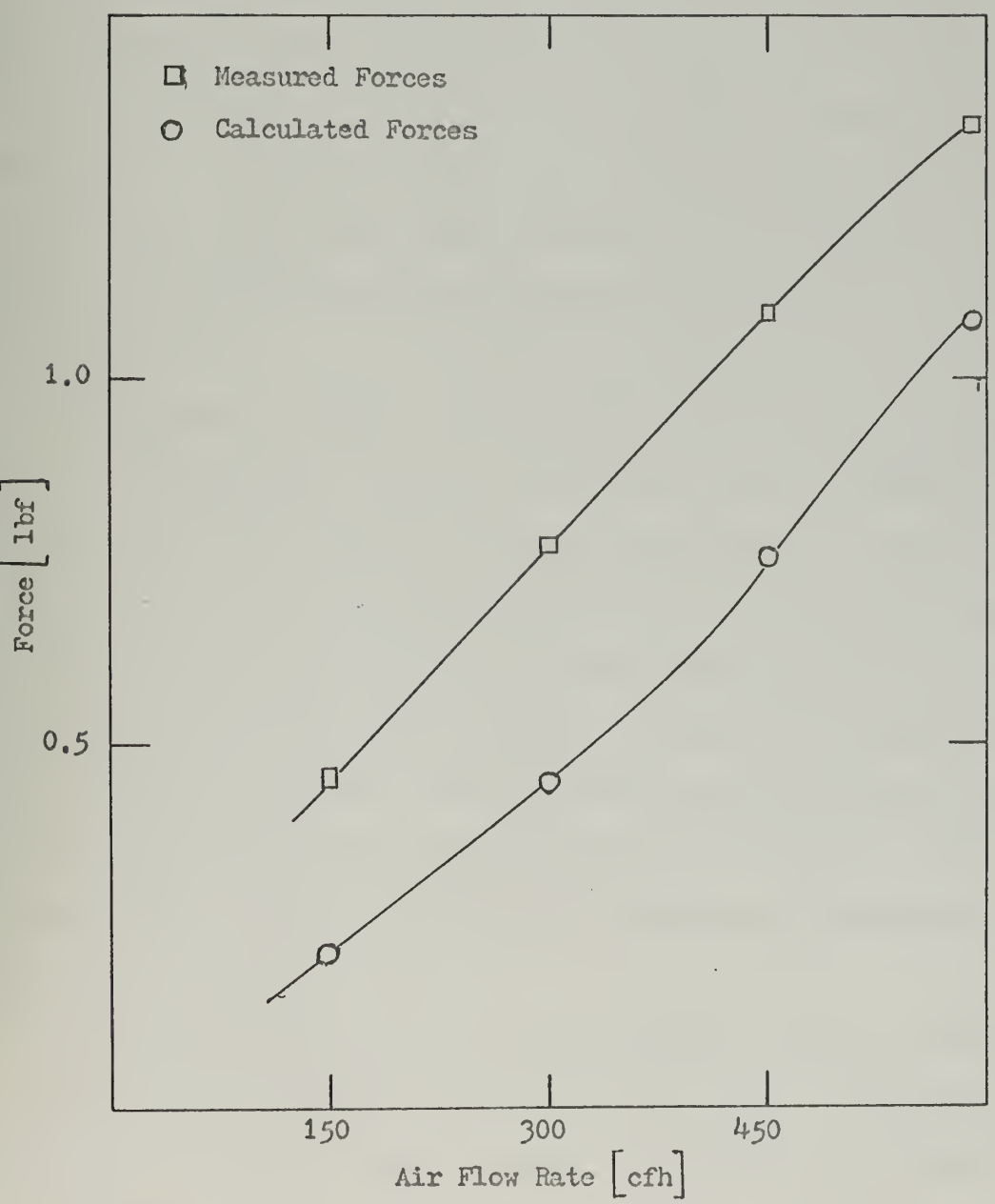

channel. From visual observation it is known that some of the flow patterns in the channel were such that at the center of the flow pattern the water was closer to the ramp than on the edges, i.e., the sides and corners were full of air and the center had relatively less. If the system is assumed to be in quasi-equilibrium, then the pressure in a bubble will be approximately constant and a flow shaped as described above would have higher pressures off the center of the ramp than on it. There were flow patterns observed which were the opposite of this, i.e., more air in the center and this would give a lower pressure off the center line. The correlation between these small flow differences and the magnitude of the difference between the measured and the calculated forces has not been fully determined.

The two curves in each plot of Figures 8 and 9 cannot be used as a source of a "calibration" factors for correcting all the integrated forces to their proper value because the pressure distribution is affected by the velocity of the model and therefore the correction factor which brings the zero velocity integrated force to the correct level is probably not the right factor to use at any other velocity. Therefore no attempt will be made to modify the integrated forces at other velocities because the modification will only bring additional confusion to the results. This lack of equality will, however, be alluded to occasionally to explain why some results appear as they do.

By inference from the fact that the inequality exists at zero velocity, it is claimed that the calculated forces for the lower velocities are probably smaller than the real forces they are to represent. In addition it is also claimed that for the smaller model (L = 4.5 ft.) the magnitude of the

difference increases with the air flow rate.

Table 4

Bollard Pull Test
Model A

Velocity 0.0 KTS

Model L = 4.5ft

Air cfh	P_1 In H_2O	P_2 In H_2O	P_3 In H_2O	P_4 In H_2O	F_I lbf	Step Corr lbf	T lbf	C_{TS}
15.0	.0456	.0320	.0076	.0322	.0447	.0052	.0449	.0081
30.0	.0763	.0681	.0190	.0577	.0760	.0100	.0766	.0138
45.0	.1013	.1066	.0363	.1101	.1151	.0191	.1172	.0211
60.0	.1295	.1493	.0565	.1363	.1447	.0242	.1480	.0266
75.0	.1372	.1372	.0733	.1823	.1620	.0316	.1677	.0302
90.0	.1498	.1934	.0871	.2357	.1922	.0416	.2021	.0364

Table 5

Bollard Pull Test
Model B

Velocity 0.0 Model L = 6.75ft

Air cfh	P_1 In H_2O	P_2 In H_2O	P_3 In H_2O	P_4 In H_2O	F_I lbf	Step Corr lbf	T lbf	C_{TS}
150	+.0228	+.0280	+.0550	+.1419	+.2073	+.0059	.2132	.0114
300	+.0222	+.0921	.0926	.3084	.4200	+.0279	.4479	.0240
449	.0945	.1701	.1201	.4820	.6842	+.0682	.7525	.0403
590	.1071	.2257	.1869	.6483	.9537	+.1235	1.0772	.0576

C. Determination of the Ramp Drag

Though the ramp drag is of little interest for itself, it is of major importance for calculating the thrust produced under self-propelled conditions.

There is no way of checking the value of the ramp drag as there was in the case of the bollard pull test. Since, however, the ramp drag is a contribution to the total model resistance and therefore to C_T, the use of $\frac{1}{2}\rho SU^2$ as a nondimensionalizing coefficient for the ramp drags might provide a basis for their comparison.

Figures 10 and 11 show the pressure distributions for both models. As with the bollard pull test, there are dissimilarities between these curves. Again P_4 is consistently higher on the large model than on the smaller one and P_1 and P_3 have exchanged positions relative to P_2 in the same manner as in the bollard pull test. This flow dissimilarity reinforces the conclusions drawn from the bollard pull test. Namely, that great care must be exercised in separating the forces which are acting in the channel so that each force is scaled in accordance with its appropriate scaling law.

Figure 12 shows the ramp drag coefficients, C_{RD}, defined as

$$C_{RD} = \frac{R_D}{\frac{1}{2}\rho SU^2}$$

plotted against Froude number. Tables 6 and 7 tabulate the original data and the values of the intermediate quantities which were calculated in obtaining C_{RD}.

Two facts are apparent. First, there is surprizingly good correlation considering the basis upon which the values were calculated. Secondly, by implication of the good correlation, the value of the force is not

Figure 10

Bare Hull Ramp Drag Pressure Distribution

as a Function of Position for Model A

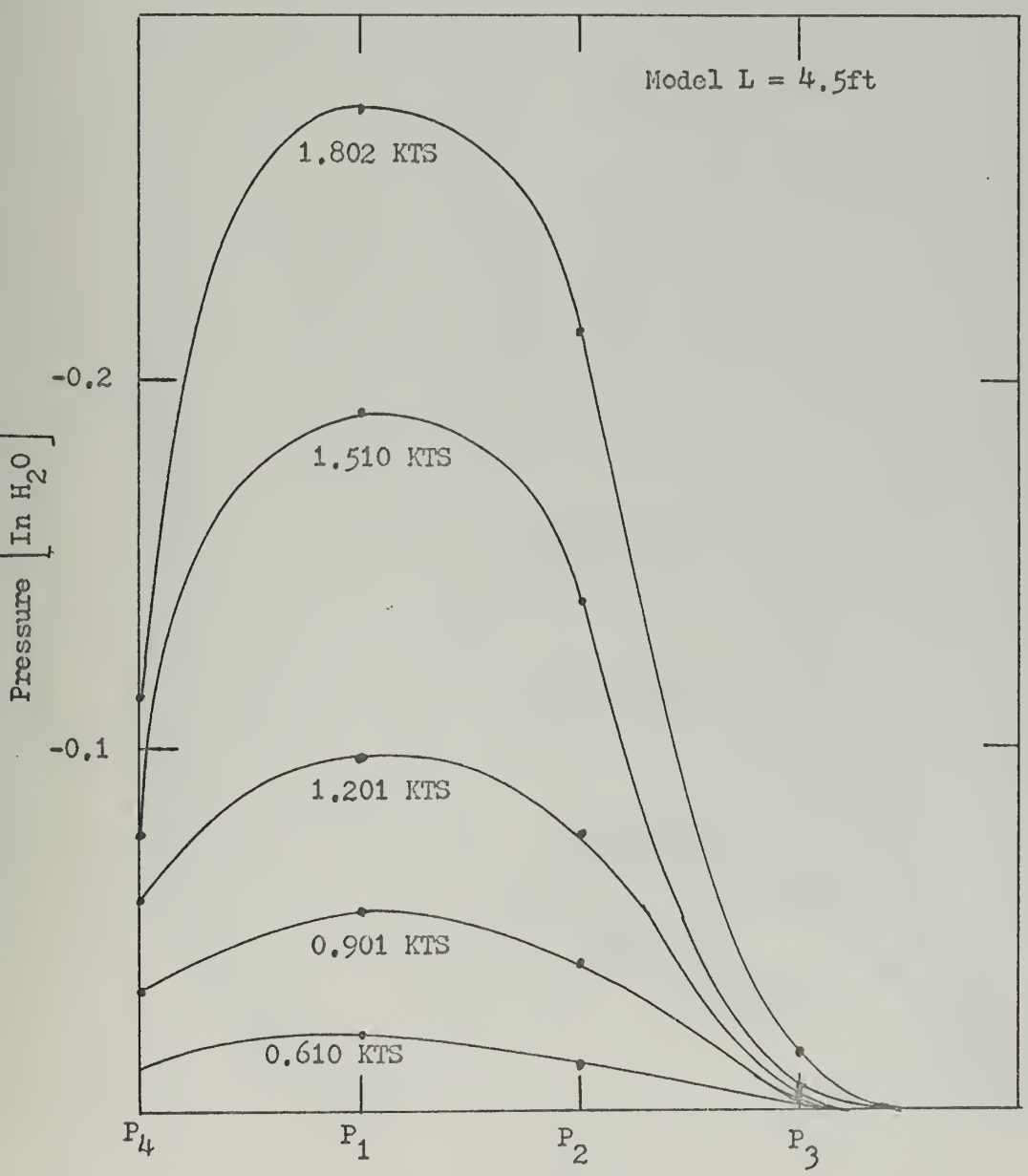

Figure 11

Bare Hull Ramp Drag Pressure Distribution

as a Function of Position for Model B

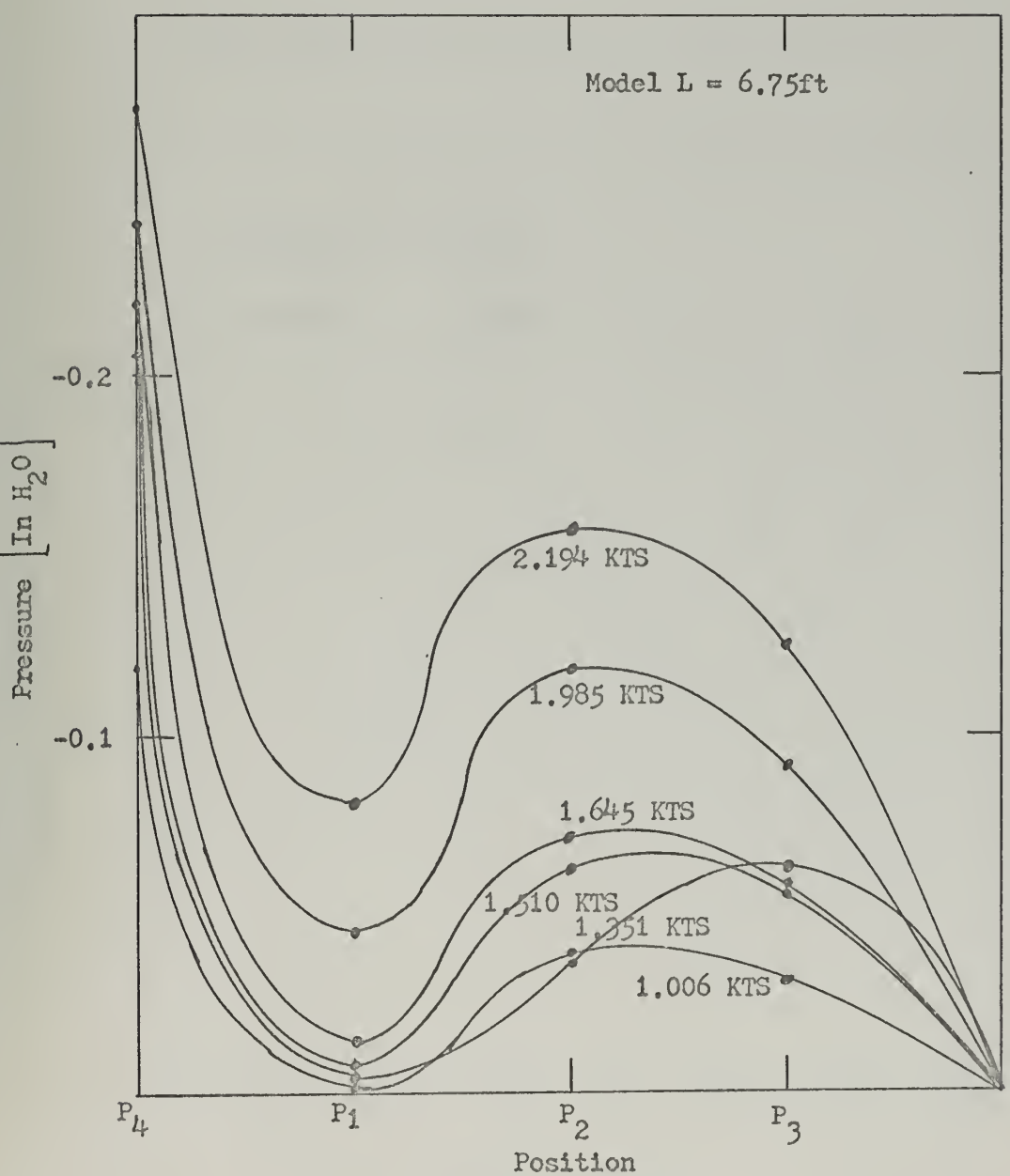

Figure 12

Ramp Drag Coefficient, C_{RD}, vs Froude Number, F

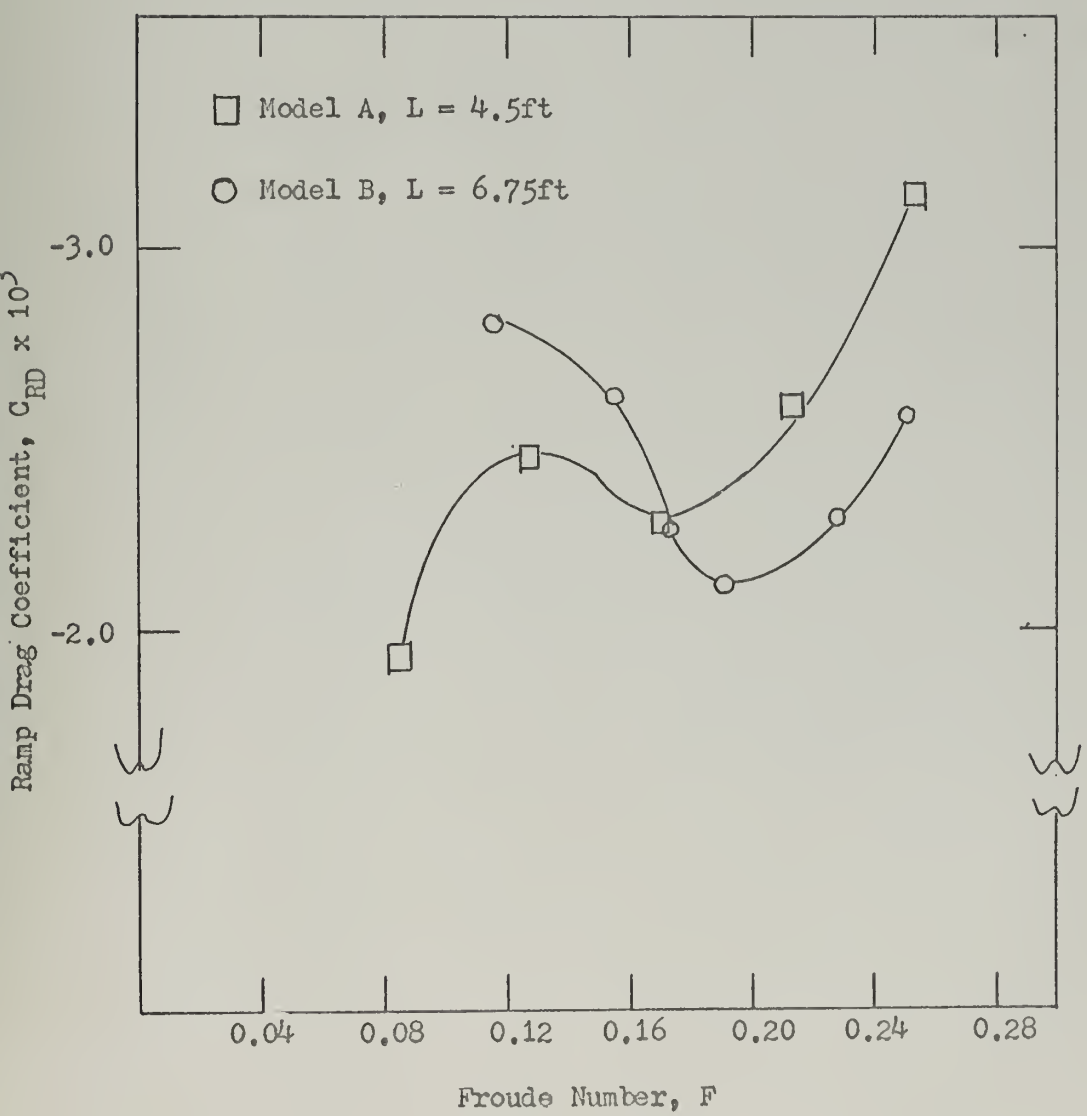

terribly sensitive to the location of the peaks and valleys. (See Figures 10 and 11.) (Later it will become apparent, however, that the value is very sensitive to the magnitude of the peaks and valleys.)

The dissimilarities between these two curves will unfortunately be reflected through the rest of the work, since the ramp drag is one contribution to the thrust calculation. This will be especially true for low thrust conditions, i.e., for low air flow rates, because at low air flow rates the calculated force which is the difference between the two large numbers is more sensitive to errors in those numbers because they are close to being equal in magnitude.

Table 6

Bare Hull Ramp Drag
Model A

Model L = 4.5ft

Froude Number	Velocity KTS	P_1 In H_2O	P_2 In H_2O	P_3 In H_2O	P_4 In H_2O	F_I lbf	Step Corr lbf	R_D lbf	C_{RD}
.0855	.610	-.0220	-.0114	0	-.0126	-.0153	0	-.0153	-.00193
.1268	.901	-.0567	-.0397	0	-.0329	-.0427	-.0002	-.0429	-.00246
.1686	1.201	-.0978	-.0761	0	-.0592	-.0699	-.0006	-.0705	-.00228
.2118	1.510	-.1921	-.1431	-.0037	-.0760	-.1250	-.0010	-.1260	-.00258
.2525	1.802	-.2753	-.2130	-.0147	-.1140	-.2171	-.0023	-.2194	-.00315

Table 7

Bare Hull Ramp Drag
Model B

Model L = 6.75ft

Froude Number	Velocity KTS	P_1 In H_2O	P_2 In H_2O	P_3 In H_2O	P_4 In H_2O	F_I lbf	Step Corr lbf	R_D lbf	C_{RD}
.1151	1.006	-.0008	-.0398	-.0314	-.1191	-.1333	-.0037	-.1370	-.00280
.1548	1.351	-.0056	-.0362	-.0628	-.1980	-.2214	-.0103	-.2317	-.00262
.1730	1.510	-.0078	-.0632	-.0562	-.2062	-.2395	-.0112	-.2507	-.00226
.1885	1.645	-.0144	-.0710	-.0576	-.2205	-.2647	-.0128	-.2775	-.00212
.2275	1.985	-.0454	-.1193	-.0916	-.2425	-.4188	-.0155	-.4343	-.00229
.2515	2.194	-.0811	-.1561	-.1256	-.2756	-.5757	-.0199	-.5956	-.00257

D. Self-Propelled Model Tests

As explained in the preceding sections on procedures, the self-propelled tests are required to provide three additional pieces of information which are:

(1) The self-propelled speed as a function of the air flow rate.

(2) The apparent resistance of the hull with air flowing, as measured by the force detectors, T_m.

(3) The pressure distribution on the ramp from which the propulsor's thrust can be calculated.

Results (1) and (2) above are produced simultaneously by simply plotting the average measured forces against the air flow rate.

Figures 13 and 14 present the average value of the measured forces. The data is tabulated in Tables 8 and 9 . The zero velocity line does not extrapolate to zero by straight line extrapolation. This indicates that very low air flow rates produce comparatively higher forces than do the higher air flow rates. This is probably the result of a change in the mechanism by which the air flow gets converted to thrust as the air flow rate increases. It has already been postulated by Kostilainen[2] that very low air flow rates should be more efficient in the sense that the incremental thrust per incremental air flow rate will be high. The reasoning is that at low air flow rates the bubbles can mix with the water better and therefore the momentum transfer is more complete. This work seems to confirm his postulate.

Taking the zero force intercept of the T_m versus air flow rate curves and nondimensionalizing the values to ϕ and F gives the values plotted in

Figure 13

Self Propelled Test: Apparent Hull Resistance, T_M, as a Function of the Air Flow Rate for Model A

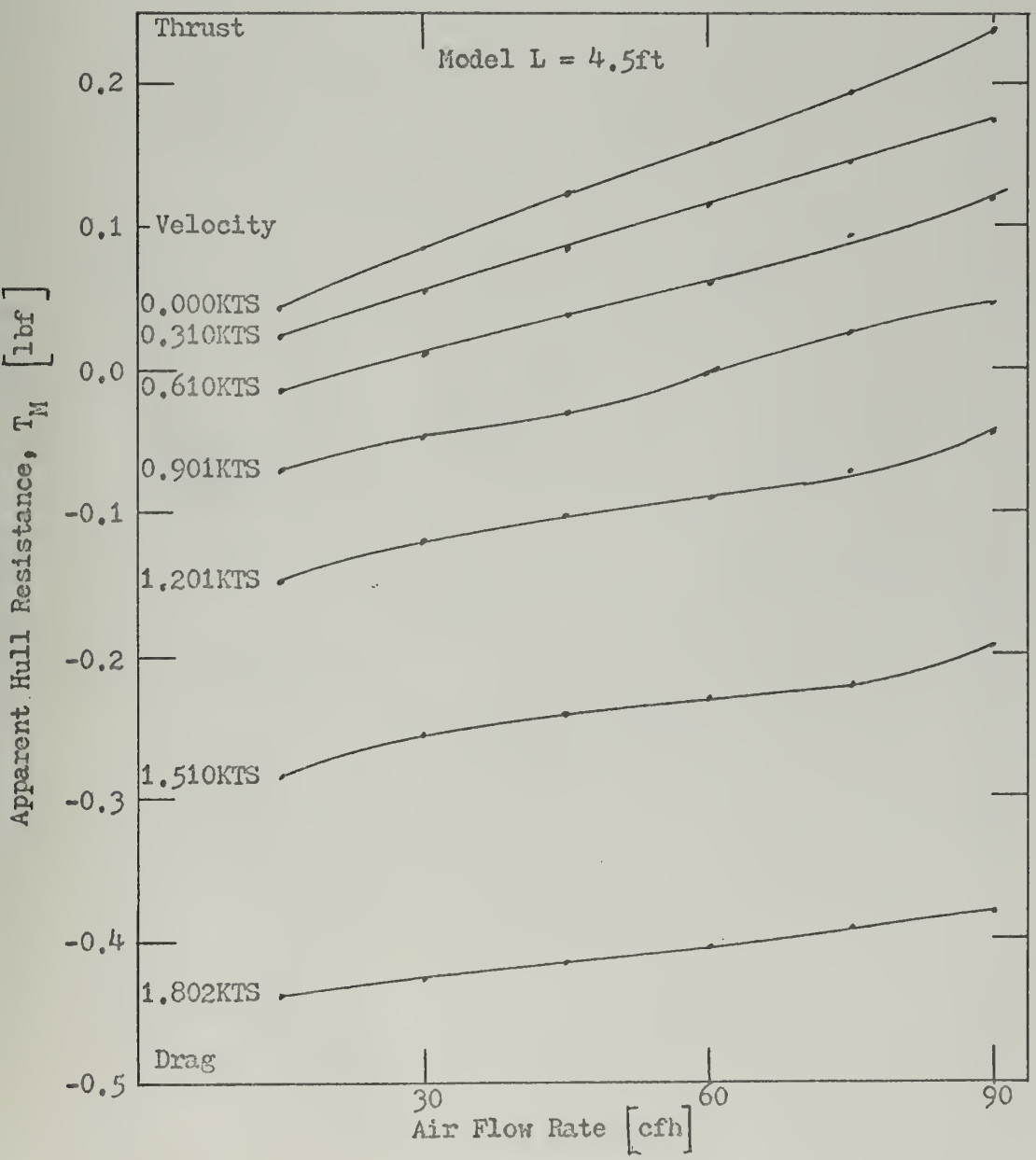

Figure 14

Self Propelled Test: Apparent Hull Resistance, T_M, as a Function of the Air Flow Rate for Model B

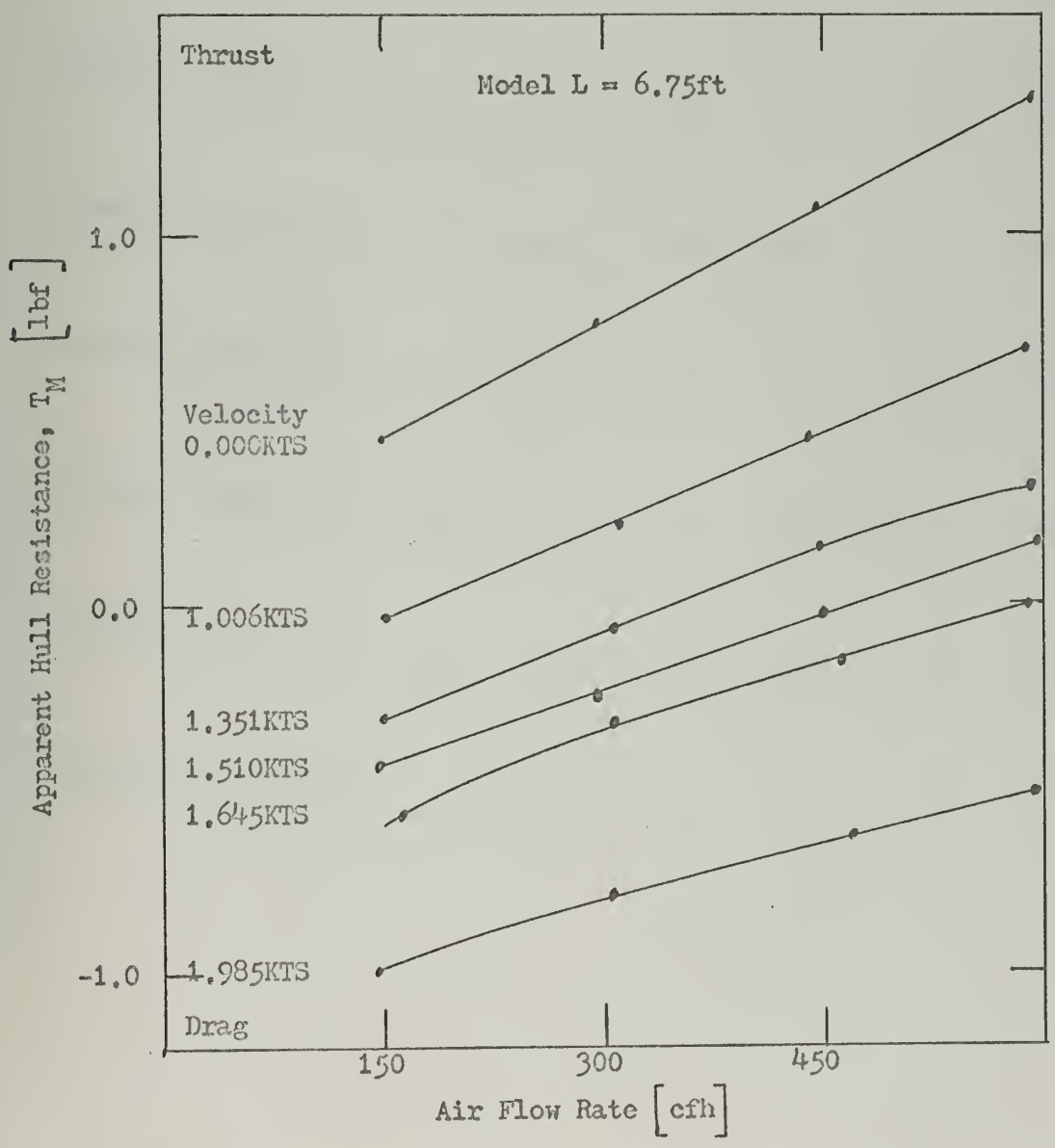

Table 8

Self Propelled Tests:
Apparent Hull Resistance, T_M
Model L = 4.5ft

Air Flow Rate [cfh]		15	30	45	60	75	90
Velocity	0.000 KTS						
	T_M [lbf]	.042	.085	.122	.159	.195	.237
Velocity	.310 KTS						
	T_M [lbf]	.023	.054	.084	.115	.145	.175
Velocity	.610 KTS						
	T_M [lbf]	-.016	.011	.038	.060	.096	.119
Velocity	.901 KTS						
	T_M [lbf]	-.070	-.049	-.031	-.002	.025	.047
Velocity	1.201 KTS						
	T_M [lbf]	-.149	-.122	-.102	-.090	-.071	-.043
Velocity	1.510 KTS						
	T_M [lbf]	-.285	-.256	-.241	-.231	-.221	-.192
Velocity	1.802 KTS						
	T_M [lbf]	-.438	-.427	-.416	-.406	-.393	-.381

Table 9

Self Propelled Tests;
Apparent Hull Resistance, T_M
Model L = 6.75ft

Velocity	0.0 KTS				
	Air Flow Rate [cfh]	148	296	445	593
	T_M [lbf]	.458	.757	1.069	1.372
Velocity	1.006 KTS				
	Air Flow Rate [cfh]	153	311	440	589
	T_M [lbf]	-.036	.205	.423	.681
Velocity	1.351 KTS				
	Air Flow Rate [cfh]	148	304	447	589
	T_M [lbf]	-.305	-.072	.154	.312
Velocity	1.510 KTS				
	Air Flow Rate [cfh]	148	296	449	593
	T_M [lbf]	-.434	-.244	-.030	.166
Velocity	1.645 KTS				
	Air Flow Rate [cfh]	163	308	460	589
	T_M [lbf]	-.569	-.315	-.147	-.004
Velocity	1.985 KTS				
	Air Flow Rate [cfh]	148	304	467	593
	T_M [lbf]	-.988	-.785	-.635	-.519

Figure 15. From this presentation of the data it is apparent that for a given Froude number (velocity) the larger model requires a higher value (air flow rate). The plot shows that the self-propelled velocity measured progress in a smooth manner and the nondimensional formulation allows both models to be plotted on the same graph. These curves are nothing more than plots of the self-propelled velocity versus the self-propelled air flow rate. Facts to remember when looking at the plot are:

(1) That the large model does actually require larger forces at a given Froude number because of the tank blockage.

(2) That the smaller model is in laminar not turbulent flow at the low Froude numbers.

(3) The change in the hull resistance resulting from the air flowing has not been separated out of the total forces yet.

Before continuing to the third set of results derived from the self-propelled tests, it should be pointed out that Kostilainen's methods of analysis are not very useful for this set of models. Figure 16 shows how C_{TA} varies with Froude number and it is apparent that the correlation is not very good, even at F = 0 where Kostilainen found good correlation on his models.

One plausible explanation for this is that for the geometry of this configuration and the air flow rates used, the nondimensional analysis and the assumption used in eliminating some variables is incorrect. The force which is most likely to be causing this is the friction force. (See Sections V.B and V.C.) The models used in this work were all tested at lower Reynolds' number than Kostilainen's models were and were therefore in a flow regime which was more dominated by friction.

Figure 15

Froude Number of the Self Propelled Velocity, F,

as a Function of Nondimensional Air Flow Rate,

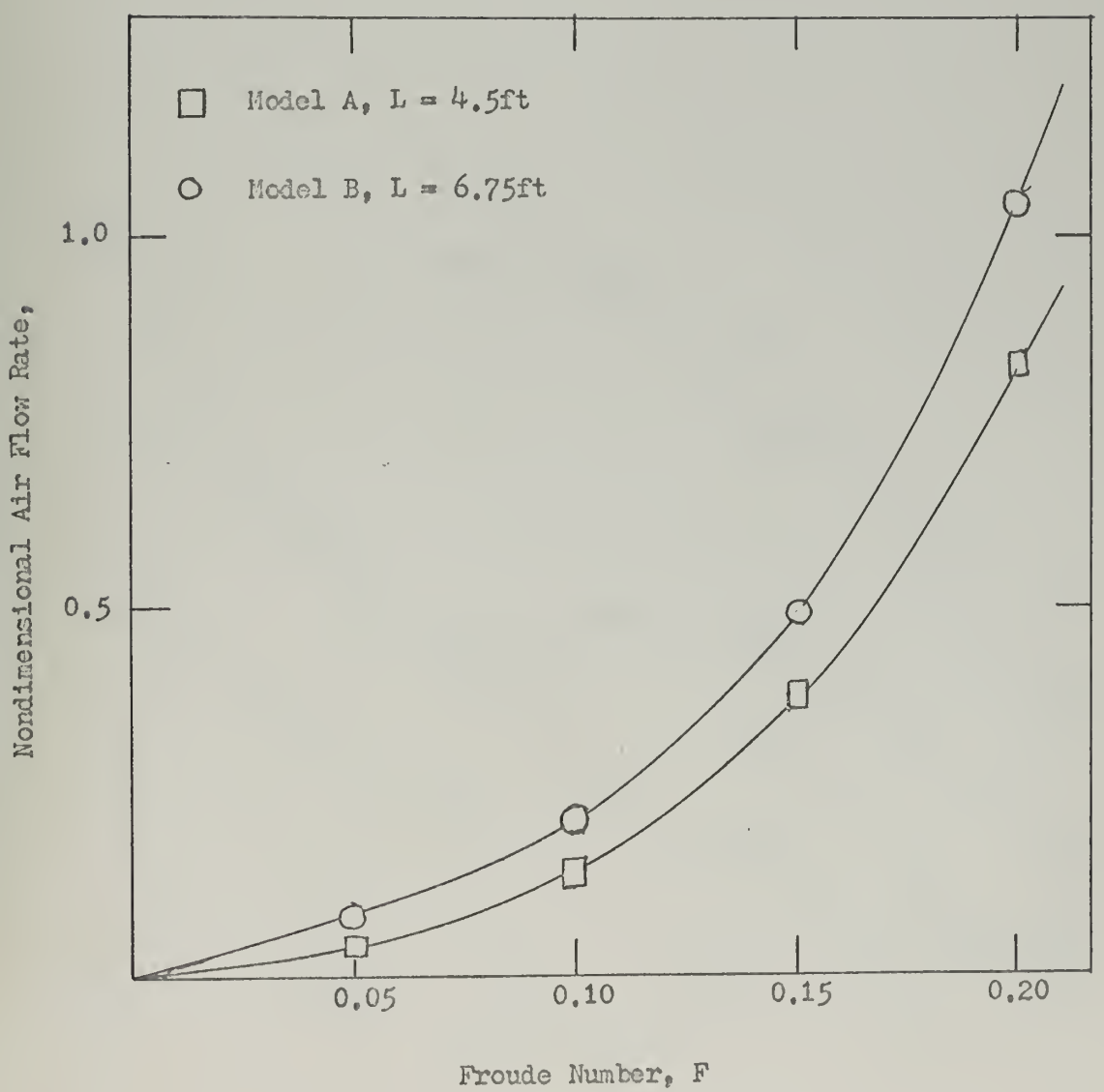

Figure 16

C_{TA} vs Froude Number, F

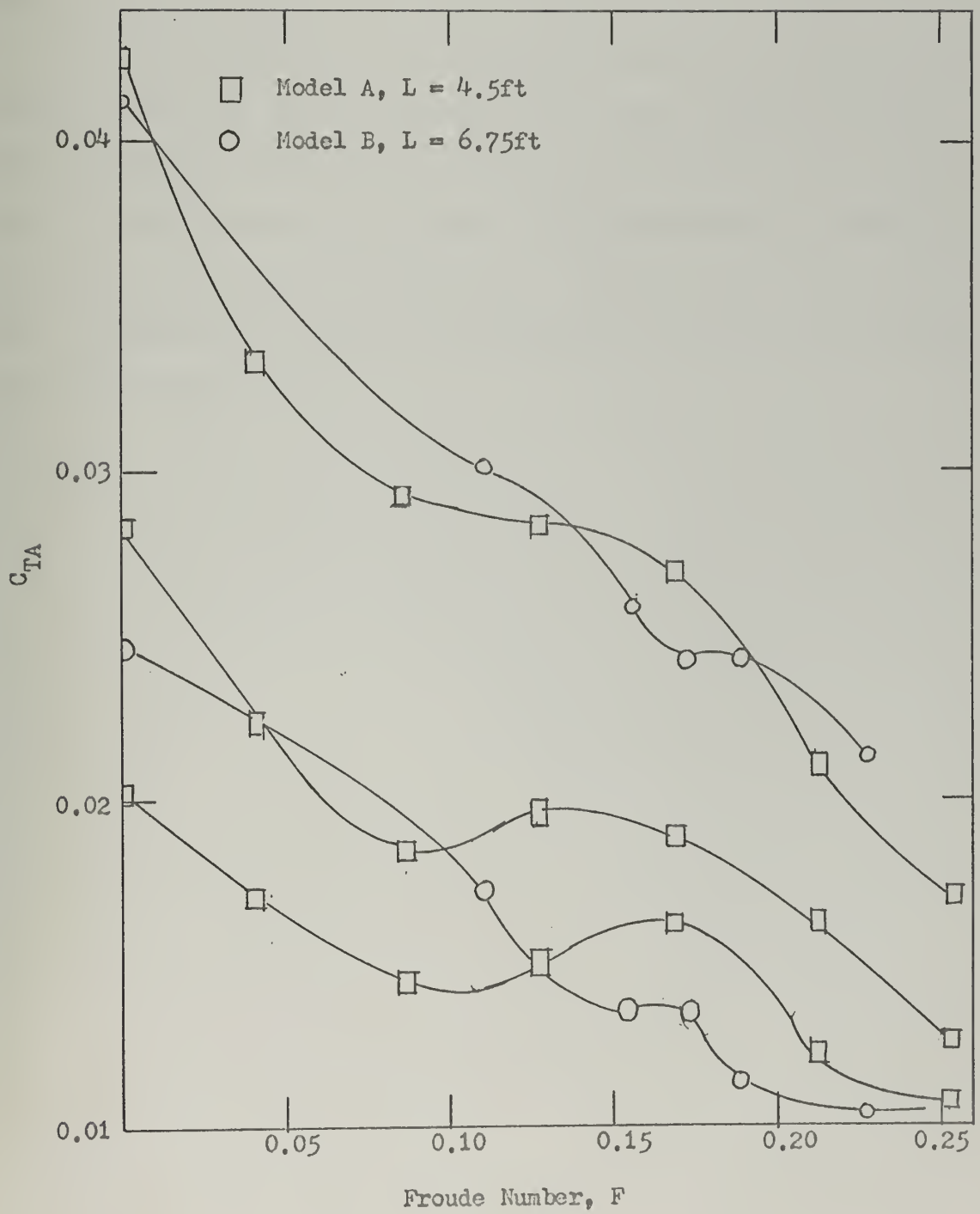

The third set of results to be extracted from the self-propelled tests is the propulsor thrust, T. Tables 10 through 27 tabulate these values and values of other quantities of interest derived from the thrust such as C_{TS} , η and C_{ϕ}.

With the exception of the fact that an increase in air flow rate is normally associated with an increase in the thrust, comparison of the thrusts with each other without nondimensionalizing them gives no new facts nor does it provide any insight into understanding the underlying principles of operation of the propulsor. Section E will take up the task of presenting the results in nondimensional form and interpreting the meaning of the plots.

Table 10

Self Propelled Model

Tests

Model L = 4.5ft — Bare Hull Resistance -.043 lbf

Velocity .610 KTS — F .0855 — Ramp Drag -.0153 lbf

Air Flow cfp	P_1 In H_2O	P_2 In H_2O	P_3 In H_2O	P_4 In H_2O	F_I lbf	Step Corr lbf	Total lbf	T lbf
14.25	-.080	-.040	.008	.028	-.0474	+.0001	-.0473	-.0298
33.25	-.043	.034	.020	-.012	.0009	0	.0009	.0184
47.5	.012	.050	.038	.003	.0283	0	.0283	.0458
61.25	.046	.043	.035	.017	.0509	.0001	.0510	.0685
76.5	.042	.090	.052	.038	.0769	.0003	.0772	.0947
91.25	.069	.129	.089	.033	.1039	.0002	.1041	.1216

Table 11

Self Propelled Model

Model L = 4.5ft — Tests — Bare Hull Resistance -.043 lbf

Velocity .610 KTS — F .0855 — Ramp Drag -.0153 lbf

Air Flow cfh	Power cut ft lb/sec	Power in ft lb/sec	η	C_{TS}	T_M lbf	$\frac{1}{2}\rho SU^2 C_T$ lbf	$\frac{1}{2}\rho SU^2 C_\phi$ lbf	C_ϕ
1425	———	———	———	———	———	———	———	———
33.25	.0190	.1156	.116	.0033	.0080	.0104	-.033	-.00411
47.5	.0472	.2697	.175	.0082	.0380	.0078	-.032	-.00444
61.25	.0706	.3853	.183	.0123	.0600	.0085	-.034	-.00435
76.5	.0976	.6205	.157	.0170	.0953	-.0006	-.044	-.00549
91.25	.1254	.7401	.169	.0219	.1193	-.0023	-.041	-.00513

Table 12

Self Propelled Model

Tests

Model L = 4.5ft

Bare Hull Resistance -.113 lbf

Velocity .901 KTS

F .1268

Ramp Drag -.0429 lbf

Air Flow cfh	P_1 In H_2O	P_2 In H_2O	P_3 In H_2O	P_4 In H_2O	F_I lbf	Step Corr lbf	Total lbf	T lbf
13.5	-.074	-.040	.008	.070	-.0391	.0008	-.0383	.0046
30.5	-.052	.008	.020	.082	-.0068	.0012	-.0056	.0373
48.75	-.028	.015	.026	.056	.0088	.0005	.0093	.0522
50.5	-.003	.042	.011	.052	.0224	.0005	.0229	.0658
77.0	.002	.043	.027	.074	.0326	.0010	.0336	.0765
92.0	.045	.060	-.007	.104	.0471	.0019	.0490	.0919

Table 13

Self Propelled Model Tests

Model L = 4.5ft — Bare Hull Resistance -.113 lbf

Velocity .901 KTS — F .1268 — Ramp Drag -.0429 lbf

Air Flow cfh	Power out ft lb/sec	Power In ft lb/sec	η	C_{TS}	T_M lbf	$\frac{1}{2}\rho SU^2C_T$ lbf	$\frac{1}{2}\rho SU^2C_\phi$ lbf	C_ϕ
13.5	.0071	.1095	.065	.0008	-.0700	.0746	-.038	-.00220
30.5	.0573	.2474	.232	.0067	-.0480	.0853	-.028	-.00159
48.75	.0802	.3954	.203	.0094	-.0307	.0829	-.030	-.00173
59.5	.1011	.4826	.209	.0118	-.0020	.0796	-.033	-.00192
77.0	.1176	.6245	.188	.0138	.0253	.0512	-.062	-.00355
92.0	.1413	.7462	.189	.0165	.0460	.0459	-.067	-.00385

Table 14

Self Propelled Model
Tests

Model L = 4.5ft

Bare Hull Resistance -.1041bf

Velocity 1.201 KTS

F .1686

Ramp Drag -.0705 lbf

Air Flow cfm	P_1 In H_2O	P_2 In H_2O	P_3 In H_2O	P_4 In H_2O	F_I lbf	Stat Corr lbf	Total lbf	T lbf
13.0	-.053	-.006	-.026	.14[illegible]	-.0714	.0036	-.0678	.0088
32.0	-.060	-.067	- 033	.104	-.0476	.0019	-.0457	.0248
[illegible]3.25	- 110	-.038	.026	.153	-.0408	.0040	-.0368	.0337
52.0	-.006	-.000	.030	.150	-.0202	.0039	-.0163	.0542
70.25	-.080	.027	.018	.175	.0134	.0045	.0179	.0884
92.0	-.048	.002	.027	195	.0139	.0067	.0206	.0911

Table 15

Self Propelled Model Tests

Model L = 4.5ft

Bare Hull Resistance -.194 lbf

Velocity 1.201 KTS

F .1686

Ramp Drag -.0705 lbf

Air Flow cfh	Power out ft lb/sec	Power in ft lb/sec	η	C_{TS}	T_M lbf	$\frac{1}{2}\rho SU^2 C_T$ lbf	$\frac{1}{2}\rho SU^2 C_\phi$ lbf	C_ϕ
13.0	.0178	.1054	.164	.0016	-.1493	.1581	-.036	-.00116
32.0	.0503	.2595	.194	.0045	-.1220	.1468	-.047	-.00153
48.25	.0684	.3913	.175	.0061	-.1020	.1357	-.058	-.00189
62.0	.1100	.5028	.219	.0098	-.0893	.1345	-.051	-.00164
79.25	.1795	.6427	.279	.0159	-.0700	.1584	-.036	-.00115
92.0	.1849	.7461	.249	.0164	-.0433	.1343	-.059	-.00193

Table 16

Self Propelled Model
Tests

Model L = 4.5ft

Bare Hull Resistance -.310 lbf

Velocity 1.510 KTS

F .2118

Ramp Drag -.1260 lbf

Air Flow cfh	P_1 In H_2O	P_2 In H_2O	P_3 In H_2O	P_4 In H_2O	F_I lbf	Step Corr lbf	Total lbf	T lbf
13.75	-.201	-.115	-.021	.101	-.1327	.0017	-.1317	-.0057
32.8	-.202	-.111	.006	.106	-.1202	.0018	-.1184	.0076
48.2	-.167	-.121	.006	.154	-.1030	.0040	-.0990	.0270
58.3	-.132	-.085	.002	.217	-.0578	.0083	-.0495	.0764
76.7	-.110	-.086	.016	.197	-.0445	.0068	-.0377	.0883
92.0	-.082	-.065	.014	.188	-.0270	.0062	-.0208	.1052

Table 17

Self Propelled Model Tests

Model L = 4.5ft — Bare Hull Resistance -.310 lbf

Velocity 1.510 KTS — F .2118 — Ramp Drag -.1260 lbf

Air Flow cfh	Power cut ft lb/sec	Power in ft lb/sec	η	C_{TS}	T_M lbf	$\frac{1}{2}\rho SU^2C_T$ lbf	$\frac{1}{2}\rho SU^2C_\phi$ lbf	C_ϕ
13.75	—	.1115	—	—	-.2847	—	—	—
32.8	.0194	.2660	.073	.0013	-.2560	.2636	-.046	-.00095
48.2	.0689	.3909	.176	.0048	-.2407	.2677	-.042	-.00087
58.3	.1950	.4728	.412	.0138	-.2313	.3077	-.0023	-.00004
76.7	.2253	.6220	.362	.0159	-.2213	.3096	+.0004	.00000
92.0	.2685	.7461	.360	.0189	-.1920	.2972	-.0128	-.00026

Table 18

Self Propelled Model

Tests

Model L = 6.75ft

Bare Hull Resistance -.352 lbf

Velocity 1.006 KTS

F .1151

Ramp Drag -.1370 lbf

Air Flow cfh	P_1 In H_2O	P_2 In H_2O	P_3 In H_2O	P_4 In H_2O	F_I lbf	Step Corr lbf	Total lbf	T lbf
153	-.0208	-.0429	-.0244	.1450	.0062	.0055	.0117	.1487
311	-.0221	-.0269	-.0167	.2274	.0595	.0136	.0731	.2101
440	-.0584	-.0208	.0465	.3567	.1948	.0335	.2283	.3653
589	-.0350	-.0147	.0908	.4757	.3245	.0595	.3840	.5210

Table 19

Self Propelled Model Tests

Model L = 6.75ft — Bare Hull Resistance -.352 lbf

Velocity 1.006 KTS — F .1151 — Ramp Drag -.1370 lbf

Air Flow cfh	Power out ft lb/sec	Power in ft lb/sec	η	C_{TS}	T_M lbf	$\frac{1}{2}\rho SU^2 C_T$ lbf	$\frac{1}{2}\rho SU^2 C_\phi$ lbf	C_ϕ
153	.2528	1.862	.136	.0080	-.036	.1847	-.1673	-.00341
311	.3571	3.785	.094	.0112	.205	.0163	-.3360	-.00684
440	.6210	5.355	.116	.0195	.423	-.0577	-.4097	-.00835
589	.8857	7.168	.124	.0279	.681	-.1600	-.512	-.01044

Table 20

Self Propelled Model Tests

Model L = 6.75ft

Bare Hull Resistance -.556 lbf

Velocity 1.351 KTS

F .1548

Ramp Drag -.2317 lbf

Air Flow cfh	P_1 In H_2O	P_2 In H_2O	P_3 In H_2O	P_4 In H_2O	F_I lbf	Step Corr lbf	Total lbf	T lbf
148	-.0286	-.0588	-.0303	.1896	-.1101	.0095	-.1006	.1311
304	-.0337	-.0343	-.0391	.2822	-.0316	.0210	-.0106	.2211
447	-.0026	-.0428	-.0251	.4057	.0852	.0436	.1286	.3603
589	-.0238	-.0282	.0461	.5336	.2306	.0750	.3056	.5373

Table 21

Self Propelled Model Tests

Model L = 6.75ft

Bare Hull Resistance -.556 lbf

Velocity 1.351 KTS

F .1548

Ramp Drag -.2317 lbf

Air Flow cfh	Power out ft lb/sec	Power in ft lb/sec	η	C_{TS}	T_M lbf	$\frac{1}{2}\rho SU^2 C_T$ lbf	$\frac{1}{2}\rho SU^2 C_\phi$ lbf	C_ϕ
148	.2993	1.801	.166	.0070	-.305	.436	-.120	-.00136
304	.5047	3.700	.136	.0118	-.072	.293	-.263	-.00298
447	.8224	5.439	.151	.0193	.154	.206	-.350	-.00396
589	1.2266	7.168	.171	.0287	.312	.225	-.333	-.00375

Table 22

Self Propelled Model
Tests

Model L = 6.75ft

Bare Hull Resistance -.683 lbf

Velocity 1.510 KTS

F .1730

Ramp Drag -.2507 lbf

Air Flow cfh	P_1 In H_2O	P_2 In H_2O	P_3 In H_2O	P_4 In H_2O	F_I lbf	Step Corr lbf	Total lbf	T lbf
148	-.0389	-.0881	-.0558	.2734	-.1146	.0197	-.0949	.1559
296	-.0260	-.0894	-.0349	.3528	-.0283	.0328	+.0045	.2552
449	-.0493	-.0306	-.0251	.4322	.0300	.0492	+.0792	.3299
593	-.0402	.0282	.0307	.4492	.1906	.0533	.2439	.4946

Table 23

Self Propelled Model Tests

Model L = 6.75ft

Bare Hull Resistance -.683 lbf

Velocity 1.510 KTS

F .1730

Ramp Drag -.2507 lbf

Air Flow cfh	Power out ft lb/sec	Power in ft lb/sec	η	C_{TS}	T_M lbf	$\frac{1}{2}\rho SU^2C_T$ lbf	$\frac{1}{2}\rho SU^2C_\phi$ lbf	C_ϕ
148	.3979	1.801	.221	.0083	-.434	.590	-.093	-.00084
296	.6512	3.602	.181	.0136	-.244	.499	-.184	-.00208
449	.8419	5.464	.154	.0176	-.030	.360	-.323	-.00293
593	1.2622	7.217	.175	.0265	.166	.329	-.354	-.00321

Table 24

Self Propelled Model Tests

Model L = 6.75ft

Bare Hull Resistance -.784 lbf

Velocity 1.645 KTS

F .1885

Ramp Drag -.2775 lbf

Air Flow cfh	P_1 In H_2O	P_2 In H_2O	P_3 In H_2O	P_4 In H_2O	F_I lbf	Step Corr lbf	Total lbf	T lbf
163	-.0286	-.0771	-.0991	.2955	-.1504	.0230	-.1274	.1501
308	-.0260	-.0771	-.0293	.3881	.0052	.0397	.0449	.3224
460	-.0415	-.0661	+.0237	.4057	.1651	.0433	.2084	.4859
589	-.0234	.0147	.0517	.4851	.2555	.0620	.3175	.5949

Table 25

Self Propelled Model Tests

Model L = 6.75ft — Bare Hull Resistance -.784 lbf

Velocity 1.645 KTS — F .1885 — Ramp Drag -.2775 lbf

Air Flow cfh	Power out ft lb/sec	Power in ft lb/sec	η	C_{TS}	T_M lbf	$\frac{1}{2}\rho SU^2 C_T$ lbf	$\frac{1}{2}\rho SU^2 C_\phi$ lbf	C_ϕ
163	.4172	1.825	.229	.0080	-.568	.718	-.066	-.00051
308	.8962	3.748	.239	.0172	-.347	.669	-.155	-.00118
460	1.351	5.598	.241	.0260	-.147	.633	-.151	-.00116
589	1.653	7.168	.231	.0318	-.004	.599	-.185	-.00142

Table 26

Self Propelled Model

Tests

Model L = 6.75ft

Bare Hull Resistance -1.189 lbf

Velocity 1.985 KTS

F .2275

Ramp Drag -.4343 lbf

Air Flow cfh	P_1 In H_2O	P_2 In H_2O	P_3 In H_2O	P_4 In H_2O	F_I lbf	Step Corr lbf	Total lbf	T lbf
148	-.0467	-.1310	-.2178	.4057	-.3722	.0433	-.3288	.1055
304	-.0558	-.1432	-.1675	.5468	-.2576	.0788	-.1788	.2555
467	-.0350	-.0981	-.0782	.5821	-.0272	.0891	.0619	.4962
589	-.0947	-.0600	.0140	.5821	.1139	.0891	.1495	.5383

Table 27

Self Propelled Model Tests

Model L = 6.75ft

Bare Hull Resistance -1.189 lbf

Velocity 1.985 KTS

F .2275

Ramp Drag -.4343 lbf

Air Flow cfh	Power out ft lb/sec	Power in ft lb/sec	η	C_{TS}	T_M lbf	$\frac{1}{2}\rho SU^2 C_T$ lbf	$\frac{1}{2}\rho SU^2 C_\phi$ lbf	C_ϕ
148	.3540	1.801	.197	.0056	-.988	1.094	-.096	-.00050
304	.8572	3.700	.232	.0137	-.785	1.040	-.149	-.00078
467	1.665	5.683	.293	.0265	-.635	1.131	-.058	-.00030
589	1.959	7.168	.273	.0312	-.519	1.103	-.086	-.00045

E. Thrust Coefficient, Air Flow Resistance Coefficient, Efficiency

The four preceding sections provide all the information needed to develop the desired output from this work, i.e., the basis for prediction of full scale ship propulsion performance using model data. The theory for accomplishing the extrapolation was outlined in Chapter III.

Kostilainen has suggested that the factor $1/\rho g B_c h^2$ be used for non-dimensionalizing and correlating results of tests on the two-phase propulsion system. As shown previously (See Chapter V. D.) this approach did not give good correlation when used to obtain C_{TA} from T_A. Figure 17 shows the results of using $1/\rho g B_c h^2$ to nondimensionalize T to yield C_{TS}. The correlation is not as good as for C_{TA} in Figure 16, but the degradation may be in part the result of inaccuracies in calculating the thrust, T. Elimination of suspicious data points did not significantly improve the situation nor did the attempt to perform a form of calibration of the thrust calculation based on using correction factors obtained by taking the ratios of the measured forces to the calculated forces in the bollard pull tests.

It must be concluded that Kostilainen's dimensional analysis is not very effective on the geometric form used for this thesis.

The approach proposed in the theory section is to obtain the hull resistance by use of C_R, C_F, and C_ϕ. C_ϕ is plotted in Figure 18. Correlation is very poor and is especially so for air flow rates above the self propelled air flow rate. This is because the values of C_ϕ are very sensitive to value of the total thrusts and some of those values are in error as was seen in Figure 9. The sensitivity comes about in the following manner. In the calculation procedure for obtaining C_ϕ one of the steps

Figure 17

C_{TS} vs Froude Number, F

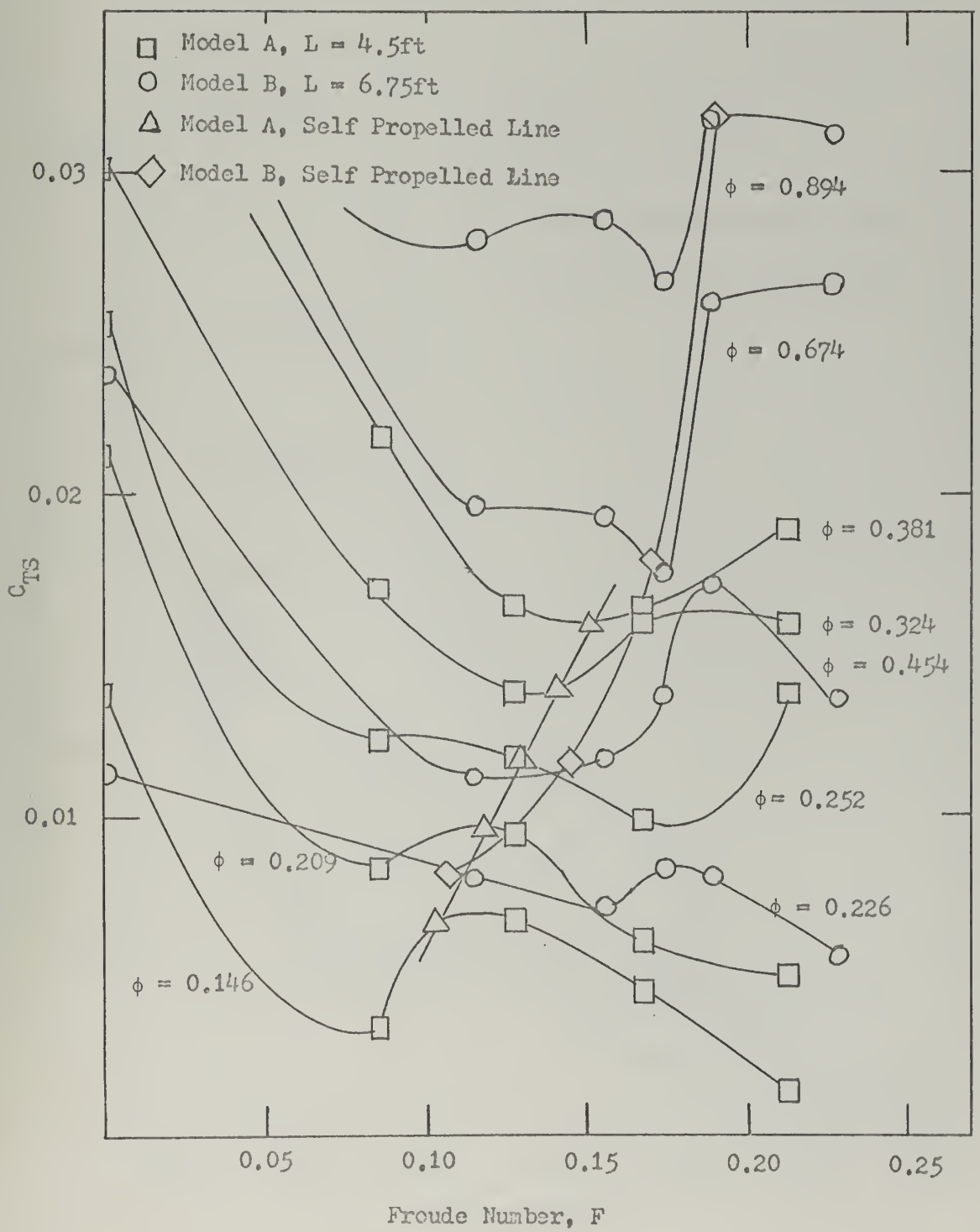

Figure 18

Air Flow Resistance Coefficient, C_ϕ , vs the Froude Number, F

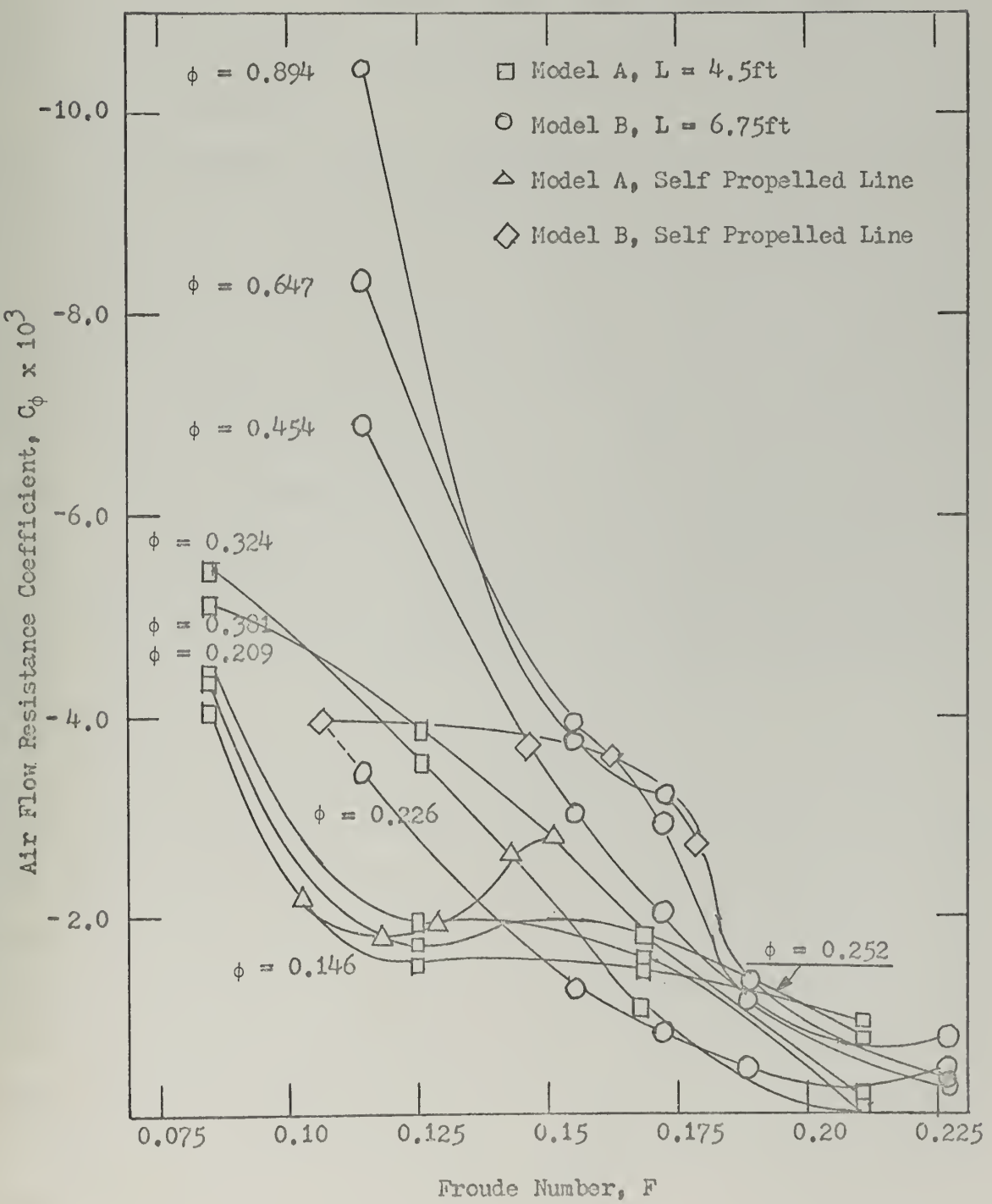

is to subtract T_m from T. At air flow rates above the self-propelled point this value should yield a positive number but because T has too small a magnitude as a result of the inadequacies of the procedure used in its calculation the difference between T and T_m becomes negative. This, of course, implies that C_T is negative, since

$$C_T = (T-T_m)/\tfrac{1}{2}\,\rho S U^2.$$

When C_{BH} is subtracted from the already negative C_T to yield C_ϕ the resultant C_ϕ is very large and negative.

Below the self propelled air flow rates the magnitude of the C_ϕ values will still be too high for any calculation which used T which was too small. Fortunately there are three curves in the plot which may be reasonably close to the correct value of C_ϕ . These curves are the C_ϕ = .146, .209 and .252 curves which correspond to air flow rates whose bollard pull test integrated force was within 10% of the measured value. These three curves cross over each other at a couple of points and one value is apparently grossly in error, but they do tend to plot along fairly closely.

The propulsor efficiency for both models is plotted in Figure 19. These values suffer from the same maladies as the two preceding quantities. Some of the points are obviously in error and can be eliminated from further consideration. Their removal can be confirmed by using the two preceding plots to help in the elimination. Unfortunately some points look "bad" only on one plot and therefore cannot be totally disregarded. The large model's data points plot lower than the L = 4.5 ft. model's data in the range of Γ = .17 and below. This is probably because the calculated forces are too low.

Figure 19

Efficiency, η, vs Froude Number, F

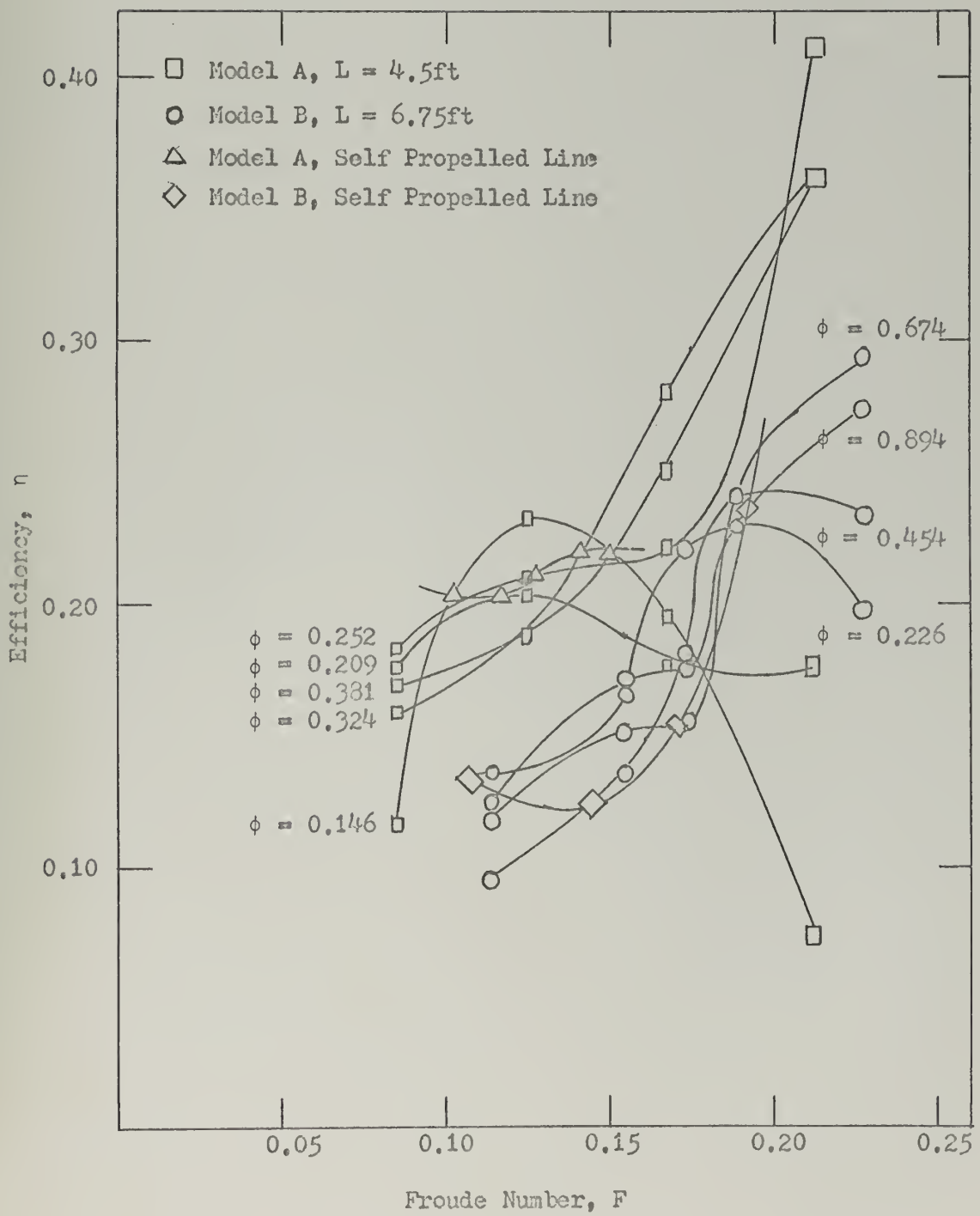

Once again three curves can probably be believed. They are the same ones as in the C_ϕ discussion, i.e., ϕ = .146, .209 and .252, and their credibility is again based on the closeness of the calculated forces and measured forces in the corresponding bollard pull tests. Based on the selection of those three curves, the efficiency can be claimed to be in the range of 20% to 22% and apparently almost independent of air flow rate.

VI. DISCUSSION AND CONCLUSIONS

The conclsuions concerning this work can logically be divided into two categories, which are those concerning the experimental techniques and equipment and those concerning the results of the investigation.

A. Equipment and Procedures

The only equipment which needs improvement is the model itself. Because the original model was of the geometry shown in Figure 2 the fol ow-on models also had its inadequacies. From the point of view of testing the model, the model has too large a beam compared to the breadth of the propulsor channel. The extra beam causes added drag, thus reducing the ship speed for a given air flow rate and therefore causes a reduction in the range of the Froude number in all plots and reduces the value of the maximum self-propelled Froude number.

The air chamber at the bottom of the channel is a waste of ship length and should be shortened. A study would be required to determine exactly how short that chamber should be and what its real effect on performance is, but, visual observation indicates that the water flow is being restrained from entering the channel at the after end of the chamber and this is probably reducing efficiency slightly.

The fact that the integrated pressures do not equal the bollard pull forces indicates that the assumption that the pressure distribution across the channel is flat is in error. Visual observation confirms the fact that air flow and water flow change as a function of the athwartships position in the channel. In part, this is a result of the fact that the air and water at the higher air flow rates do not mix very well. A new orifice

system might improve the mixing and thereby raise the efficiency of the propulsor.

One possible way of increasing the mixing of the air and water would be to increase the air velocity leaving the orifice. Of course this would also increase the orifice losses which would tend to reduce the efficiency, but a trade-off study could be made to find the optimum air flow rate and air velocity condition.

It should be pointed out that items discussed above are not going to result in major changes in the efficiency of the two-phase propulsion system.

The major procedureal inadequacy of this work results from the selection of the option of calculating the thrust from the pressure distribution vice direct measurement. It was a poor selection for two reasons, the first being that the pressure distribution is not flat across the channel. In addition to that, the athwartships distribution is probably not the same at the bottom of the ship as it is at the stern; therefore, to measure the pressure accurately would require a large number of pressure transducers and would still probably not be exact or even as accurate as a direct force measurement.

The second reason that measurement of pressures is a poor tool in this application is that the pressures are highly oscillatory and produce highly oscillatory forces thus requiring averaging and thereby introduce errors into the calculations. A significant improvement would be made by finding a method for taking longer samples that could yield better average values. Placing the propulsor in a flow channel would accomplish this.

Therefore it is concluded that:

(1) A new geometry be determined for the model;

(2) The ramp be designed in a manner which will allow direct measurement of the thrust;

(3) The measurement of the thrust be accomplished in a flow channel.

These changes will improve the accuracy of the results and shorten the length of time required to make the measurements and obtain the data needed.

B. Results

The results of this investigation are such that few conclusions concerning the original objectives can be drawn from them. It is obvious that many of the points in the plots are in error. The fact that the integrated forces do not generally equal the measured forces in the bollard pull tests indicates that besides the random errors from mistakes and from the inaccuracies of taking averages of oscillating variables, there is also a systematic error of considerable magnitude. As noted previously, this systematic error probably arises from the erroneous assumption that the pressure distribution is not a function of the athwartships position.

Some encouragement can be taken from the fact that when the obviously bad results are disregarded, the curves have the same general shape and that where they predict nonsense the reasons for the poor quality of results can be explained.

The plot of C_{TS} versus F, Figure 17, gives the best proof that all the forces involved in the two-phase propulsion system are not being properly scaled by techniques similar to those of Kostilainen. This conclusion is

based on the obviously poor correlation between models.

The plots of C_ϕ and η versus F, Figures 18 and 19 are too badly confused with inaccuracies to allow any definite conclusions to be drawn concerning whether or not they represent the correct way to scale the two-phase propulsion system. Both sets of results give some encouragement though. Throwing out the obviously bad points, the curves tend to agree with physical reasoning. For example, C_ϕ, displays a behavior which could be explained as follows. As the velocity of a vessel increases to higher values, the ability of a fixed air flow rate to reduce the hull resistance decreases because the increase in water turbulence will increase the probability of water penetrating the layer of air and thereby contacting the hul and thus increase the momentum transfer from the hull to the water and therefore raise the resistance. This would imply that C_ϕ (being negative) should move toward positive values with increasing F, and it does. Even the "bad" points don't significantly violate this trend.

It can be concluded that the C_ϕ and η approach to scaling have not been proven to be useless and may be quite good. Better data is needed before a stronger declaration can be made.

Another conclusion which can be drawn from this work is that the efficiency is poor enough so that the two-phase propulsion system will not be economically competitive with a displacement ship with a screw. The poor propulsor efficiency will require that extra fuel be provided which increases operating costs and reduces cargo carrying capabilities. Additionally, it is apparent from the pictures and the lines drawings that for its length it has a relatively small cargo space available, thus increasing the initial procurement cost/pound of payload figure. Therefore, on a volume

limited ship design project, this propulsion system will be of little value. Some gains in maintenance costs may be available but the considerations above will probably disqualify any such gains.

In summary, it is concluded that:

(1) The two-phase propulsion system configuration used for this work is not very efficient at the air flow rates and velocities measured.

(2) The scaling law postulated in Chapter III is a potentially useful calculational tool and represents an approach to the scaling problem which may ultimately be successful.

(3) Further work should be conducted on the two-phase propulsion system in accordance with the suggestions in the next chapter.

VII. APPLICATION, ENGINEERING CONSIDERATIONS AND SUGGESTIONS

There are many other aspects of the two-phase propulsion system which must be considered in making a judgement concerning its future usefulness besides the fact that it is not very efficient and will probably have a total life cycle cost which is well above that of a conventional screw propulsion system.

Of considerable importance is the problem of backing down. The device has no way by itself of creating a backing force. Therefore it would require some additional device for that purpose. Kostilainen's self-propelled model solved this problem by providing a ramp on the forward part of the vessel to which the air could be ducted and thus provide a backing force. Though that solution was satisfactory for a research device it would not be practical for commercial cargo-type vessels as it further reduces the space available for cargo.

Closely coupled to the backing problem is a concern for the vessel's maneuvering capabilities. Most vessels which require any significant capability in this respect have rudders which are in the propeller wash. Because of the highly oscillatory nature of the flow, placement of the rudder in the propulsor wash could result in a need for the rudder to withstand very high force levels. Placement of rudders on the trailing edge of the skegs will undoubtedly be the most practical method of control but will probably not result in very good control characteristics.

The highly oscillatory nature of the force was quite evident at high air flow rates. Under those conditions the models experienced considerable surging and pitching. If a full-sized ship were forced to undergo such

surging and pitching it would be a very uncomfortable ship to ride and might possibly need structural reinforcement to be able to withstand the effects of stress and fatigue.

Measurements of the pressures on the ramp indicated that for the smaller (L = 4.5 ft.) model at high air flow rates the peak pressures were commonly as much as twenty times the average. This means that the ramp experienced a pounding force which was approximately one-sixth of the static head. This situation seems to compare to cavitation which can cause severe erosion damage.

The two-phase propulsion system does have some unique features which may ultimately result in its practical application. One is the lack of an external screw. A second is that the engine and fan installation would be much lighter than that of a conventional power plant.

One area of application where efficiency is of little importance is the use of this device as a lateral thrust unit. It could be used on the surface to provide thrusts for keeping ships from putting too much strain on mooring lines in high crosswinds by placing a ramp device with camels outboard of the ship.

Along the same lines another possible use of this device might be in providing thrust for moving and holding or dislodging objects during shallow water salvage, repair or construction operations. Ramps could be lowered to the bottom and attached to the object to receive the thrust and then through the use of compressed air supplied through hoses, the device could be operated and controlled.

It might be possible to use the device on small barges which are towed in long lines by a tug. Slight modification of each barge and installation

of one of these devices could reduce the towing power requirements of the tug thus allowing it to tow longer lines of barges and possibly reduce the overall cost.

Continued study of the two-phase propulsion system is recommended but the impetus for such work should not arise from an interest in immediate application to ship propulsion, unless one of the special features of the system is anticipated to be particularly useful. There is, however, considerable ground for academic interest and for work aimedat establishment of fundamental information and also for establishing some of the properties of the system which have not been measured.

One area of study which is quite general and certainly needs some emphasis is the measurement of forces whose oscillations are of about the same magnitude as the average. In the special case of the two-phase propulsor, it might be possible to design a force block to attach to a floating ramp which has one (fore and aft) degree of freedom but is sealed for watertight integrity.

There are quite a number of aspects of this propulsion system which have not been looked at yet. One such aspect is alternate configurations. It would be nice to have a theory which was definitive enough to present some suggestions to the experimenter on how to optimize the system through geometric variation; however, none exists. Alternate configurations must be approached then from the point of view of applying sound engineering principles to the system and establishing what parameters might have the greatest effect. Some of these changes are: the ramp angle, the shape of the stern, the number and location of orifices and the shape of the ramp.

Two aspects of the flow that have not as yet been studied are: what happens to the forces when the water flow is in opposition to the bubble motion and what is the effect of constraints such as low clearance between the bottom of the hull and the bottom of the body of water.

Though it has been stated before, it bears repeating that any future work on this propulsion system should not try to measure the thrust by pressure integration until direct measurement techniques have been shown to be inadequate.

BIBLIOGRAPHY

1. S. Schuster, et al., "Uber Probleme des Wasserstrahlantriebs," Jahrbuch der Schiffbautechnischen Gessellschaft, Springe=Verlag, Berlin/Goetlingen/Heidelberg, 1961.

2. V. Kostilainen, "Two-Phase Air-Water Propulsion System Based on the Gravity Effects," Finland Institute of Technology Shipbuilding Laboratory, Report No. 3, published in International Shipbuilding Progress, Vol. 15, September 1968, No. 169.

3. V. Kostilainen, I.J. Sukselainen and T. Lindberg, "Experiments on Scale Effect and Bubble Formation in Two-Phase Propulsion." Helsinki University of Technology Ship Hydrodynamics Laboratory, Otaniemi, Finland, 1970.

4. J. P. Comstock (editor), Principles of Naval Architecture, The Society of Naval Architects and Marine Engineers, New York, 1967.

5. J. R. Scott, "On Blockage Correction and Extrapolation to Smooth Ship Resistance," Trans. SNAME, Vol. 78, 1970.

6. E. Silberman, Production of Bubbles by the Disintegration of Gas Jets in Liquid, 5th Northwest Conference on Fluid Mechanics, Ann Arbor, 1957.

APPENDIX A

Kostilainen[2, 3] has performed a dimensional analysis; a momentum balance and an energy balance on a two-phase propulsion system. A summary of the analysis is included in this appendix for easy reference. It should be noted that the notation used in the following paragraphs is the one defined in the main body of this thesis and not Kostilainen's original notation. In addition, he deals with a slightly different geometry than the one used in this thesis. The main differences are that the orifices of models A and B are the full width of the channel, while Kostilainen's models had several round orifices evenly distributed across the channel, and Kostilainen's models do not have an air chamber.

For his dimensional analysis Kostilainen selected as a starting point an equation of the form:

$$\frac{T}{B_c} = f(\rho, U_L, V_G, N_B, \delta_o, h, g, \mu, \sigma)$$

where

N_B = number of orifices per unit width

δ_o = diameter of an orifice

μ = viscosity of the liquid

σ = surface tension of the liquid

Using the Buckingham π theorem he eliminates ρ, g and h. He then presents arguments based on Silberman's[6] results which allow him to neglect the dependence of T/B_c on σ and μ. He then selects

$$C_{TS} = \frac{T}{\rho g B_c h^2}$$

$$\phi_K = \frac{\dot{V}_G}{B_c h\sqrt{gh}}$$

and

$$F_{nh} = \frac{UL}{\sqrt{gh}}$$

partly based on the fact that these coefficients gave him the best correlation of data. ϕ_K is a dimensionless air flow rate and F_{nh} is a modified Froude number.

To obtain a momentum balance he has selected a control volume as seen in Figure 20. Using the velocities as shown there (U_G is the outflow velocity of the gas and U_2 the velocity of the two-phase flow at the water surface) and defining V_L as the amount of liquid that gets accelerated, and β as the angle the ramp makes with the water surface, conservation of momentum then gives the thrust

$$T = \rho V_L (U_2 - U_L) \cos \beta$$

where gas momentum has been neglected. For his energy considerations he defines an efficiency, η_J, which is the ratio of the increase of kinetic energy of the liquid to the loss of potential energy of the gas. Then

$$\eta_J = \frac{1}{2gh} \frac{V_L}{V_G} (U_2^2 - U_L^2).$$

Combining these two results he shows that

$$T = \eta_J \frac{2\rho V_G gh}{U + U_2} \cos \beta$$

This could be nondimensionalized.

Though this has resulted in a rather simple algebraic expression it has not made experimentation any easier because η_J is not a directly measurable quantity and U_2 is at best difficult to measure.

APPENDIX B.

The following is a numerical example of the calculation performed on each self-propelled velocity-air flow rate combination. (See Tables 18 and 19 .)

Model: L = 6.75 ft.

Velocity = U = 1.006 KTS

$F = U/\sqrt{gL} = .0678 \times 1.006 = .1151$

Air Flow Rate = 440 [cfh] (average of several runs)

$$\phi = \frac{\text{Air Flow Rate}}{L^2\sqrt{gL}} = .001489 \times 440 = .655$$

Simpson's Rule for calculating the area under a curve applied to P_1, P_2, P_3 and P_4 yields the following equation.

F_I = force on the ramp parallel to the ship's axis.

$$F_I = \frac{\text{Ramp area} \times \sin\beta}{3}(P_4 + 4P_1 + 2P_2 + 4P_3) \quad .0360 \frac{\text{psi}}{\text{in } H_2O}^{*}$$

$\therefore F_I = (.7282)(.2675) = .1948$ lbf

$$\text{Step Corr} = \frac{.0360 \text{ psi}}{\text{in } H_2O} \times \frac{B_C \Delta P_4^2}{1.5} = .2631\ P_4^2 = .0335 \text{ lbf}$$

Total = F_I + Step Corr = .2283 lbf

Thrust = T = Total - Ramp Drag = .3653 lbf

Look up ramp drag in Table 7 .

$$\text{Power in} = V_G \cdot \rho gh = .0122\ V_G[\text{cfh}] = 5.335 \frac{\text{ft lbf}}{\text{sec}}$$

$$\text{Power out} = T \cdot U = (.3653 \text{ lbf})(1.700 \frac{\text{ft}}{\text{sec}}) = .621 \frac{\text{ft lbf}}{\text{sec}}$$

*The small model was calculated slightly differently. See end of this Appendix.

$$\eta = \frac{\text{Power Out}}{\text{Power In}} = \frac{.621}{5.335} = .116$$

$$C_{TS} = \frac{T}{\rho g B_C h^2} = \frac{.3653}{18.69} = .0195$$

T_m is taken from Figure 17.

$\frac{1}{2}\rho SU^2 C_T = T - T_m = .3653 - .423 = - .0577$ lbf

$\frac{1}{2}\rho SU^2 C_\phi = \frac{1}{2}\rho SU^2 C_T - \frac{1}{2}\rho SU^2 C_{BH}$

$\frac{1}{2}\rho SU^2 C_{BH}$ = Bare Hull Resistance

C_{BH} is taken from Table 3.

Therefore:

$\frac{1}{2}\rho SU^2 C_\phi = - .0577 - .352 = - .4097$ lbf

$$C_\phi = \frac{-.4097 \text{ lbf}}{49.07 \text{ lbf}} = -.00835$$

For the smaller model (L = 4.5 ft.) the pressures, P_1, P_2, P_3 and P_4 were plotted and a smooth curve was drawn through the points. Simpson's Rule was then applied to that curve and was based on a twelve divisions vice the four divisions displayed above. The thrusts obtained by making the extra plot are within a few percent of the much simpler procedure used above and therefore it was not used for the larger model calculations.

The bollard pull forces and the ramp drag forces were calculated using applicable sections of the above procedure. See Tables 4, 5, 6, and 7.

Figure 20

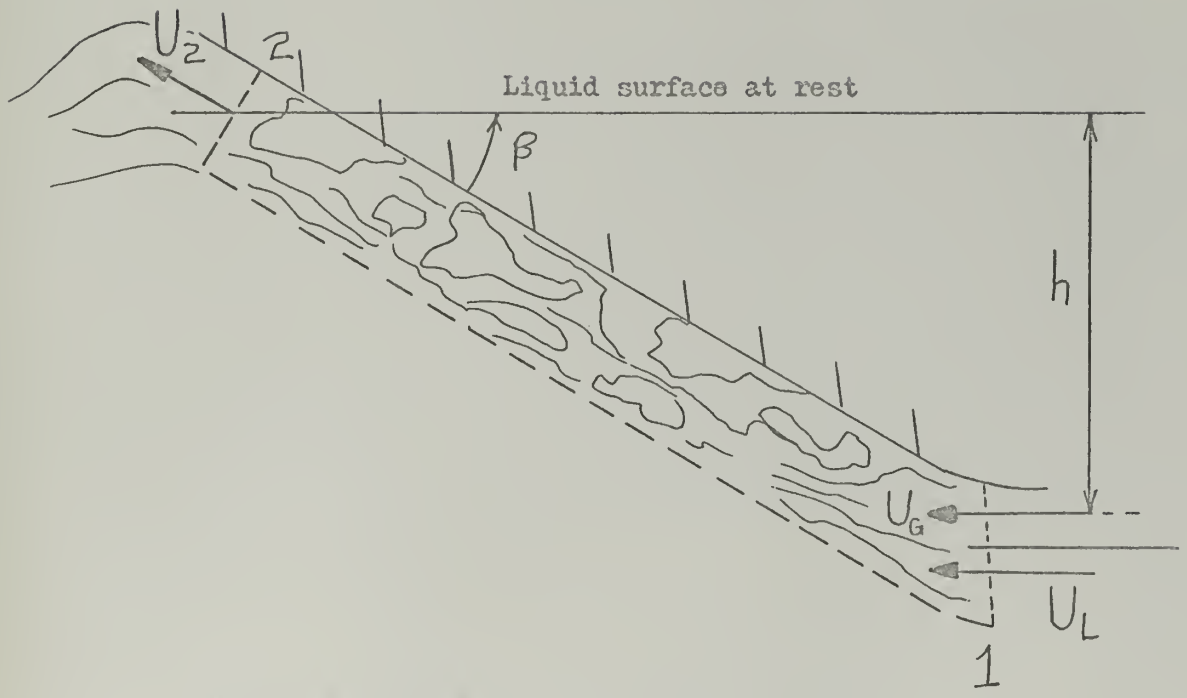

Momentum Balance for a Two-Phase Propulsor

Finally, the efficiency of the system, η, (exclusive of piping, etc.) he expresses by the following equation:

$$\eta = \frac{T\ U_L}{\rho V_G g h} = \frac{F_{nh}}{\phi_K} C_{TS} .$$

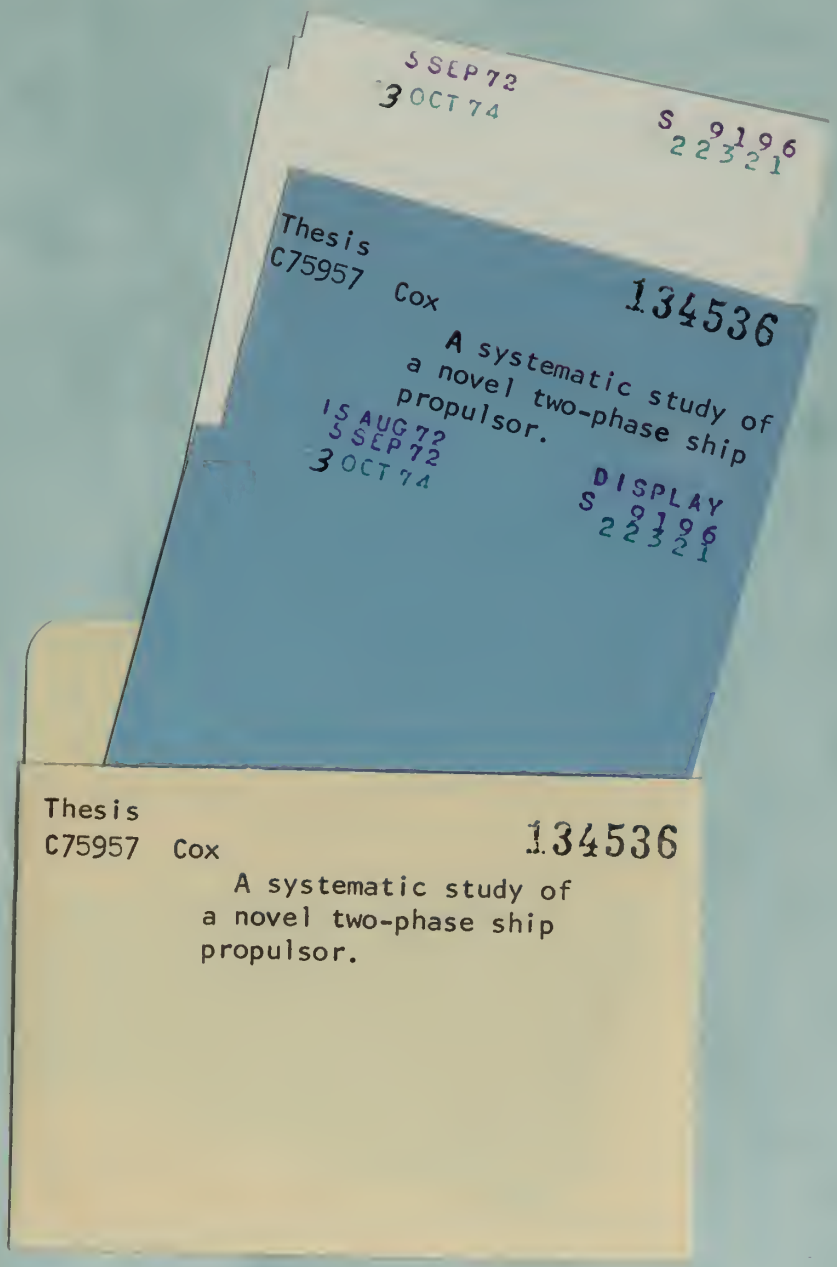
5 SEP 72
3 OCT 74
S 9196
22321
Thesis
C75957 Cox
134536
A systematic study of a novel two-phase ship propulsor.
15 AUG 72
5 SEP 72
3 OCT 74
DISPLAY
S 9196
22321
Thesis
C75957 Cox
134536
A systematic study of a novel two-phase ship propulsor.

thesC75957
A systematic study of a novel two-phase
3 2768 002 09029 2
DUDLEY KNOX LIBRARY